NASA CONTRACTOR REPORT

NASA CR-312

STUDY ON THE ELECTRON IRRADIATION EFFECTS ON CAPACITOR-TYPE MICROMETEOROID DETECTORS

Prepared under Contract No. NAS 1-3892 *by*
RESEARCH TRIANGLE INSTITUTE
Durham, N. C.
for

NATIONAL AERONAUTICS AND SPACE ADMINISTRATION • WASHINGTON, D. C. • OCTOBER 1965

NASA CR-312

STUDY ON THE ELECTRON IRRADIATION EFFECTS ON CAPACITOR-TYPE MICROMETEOROID DETECTORS

Prepared under Contract No. NAS 1-3892 by
RESEARCH TRIANGLE INSTITUTE
Durham, N.C.

for

NATIONAL AERONAUTICS AND SPACE ADMINISTRATION

For sale by the Clearinghouse for Federal Scientific and Technical Information
Springfield, Virginia 22151 – Price $3.00

Foreword

This report was prepared by the Research Triangle Institute, Durham, North Carolina, on NASA Contract NAS1-3892 "Theoretical Study on the Electron Irradiation Effects on Capacitor-Type Micrometeoroid Detectors".

This investigation began in May 1964 and was concluded in May 1965. It was performed by the Solid State Laboratory of the Research Triangle Institute under the general direction of Dr. R. M. Burger. While L. K. Monteith was the author of this report, the entire technical staff has participated to some degree in this effort. Specific credits are due T. M. Royal and H. B. Lyon for their invaluable contributions in this investigation.

This report is directly related to an earlier report "Theoretical Analysis of Operational Characteristics of Micrometeoroid Capacitor Detectors" dated April 1964 prepared under Contract NAS1-3343 (CR-56316).

Table of Contents

List of Illustrations

List of Illustrations (Continued)

Chapter I

Introduction and Summary

The purpose of this investigation is to develop a phenomenological understanding of the effects associated with electron irradiation of a capacitor-type micrometeoroid detector. A previous study under Contract NAS1-3343 which resulted in the report "Theoretical Analysis of Operational Characteristics of Micrometeoroid Capacitor Detector" dated April 1964, outlined those areas where detailed knowledge concerning ambiguous signal generation was lacking. This outline centered around two major aspects of the problem: (1) charge storage in the dielectric region of the capacitor structure, and (2) spontaneous discharge resulting from electron irradiation.

The present work has shown that electron irradiation of capacitor type structures consisting of polyethylene terephthalate films with thin aluminum electrodes results in a trapped charge distribution in the dielectric region. The decay of the trapped irradiation electrons has been detected and shown to be consistent with a no-retrapping release model based upon a density of traps that is uniform with respect to energy measured from the conduction band. A minimum value of 1.7×10^{16} per cm^3 per ev has been determined for the trap density.

A saturation effect for irradiation electron trapping has also been noted. Based upon the model used to describe the observations, a value of 4.25×10^{15} electrons/cm^3 resulting in a maximum value of built-in electric field of 5×10^5 volts/cm has been inferred. This is approximately an order of magnitude below quoted values for the field strength

of the material. The trapped charge which results in the built-in field decays to 1/2 the initial value after ceasing the irradiation in approximately 48 seconds. Reproducible results without any evidence of residual charging can be obtained if the decay of trapped charge is observed for at least 10^3 seconds after each irradiation.

Irradiation of the capacitor type structure using a beta source, Promethium 147, has resulted in spontaneous discharge. The average value of the discharge pulse height for 668 pulses was 72 millivolts while the maximum value was 2.7 volts. The pulse is an exponential decay from its maximum amplitude as predicted by theoretical considerations. Finally the origin of the breakdown is investigated. All observations lead to the conclusion that breakdown initiated by the electrical field resulting from the trapping of irradiation electrons primarily occurs at defects in the polyethylene terephthalate film and in most instances does not liberate all the trapped charge.

Chapter II

Trapping and Thermal Release of Irradiation Electrons from Polyethylene Terephthalate Films

2.1 Introduction

Electron irradiation effects in solids are usually classified in terms of ionizing events and atomic displacements. For metals and semiconductors the identity of the irradiation electrons is characterized in terms of the energy given up in these events. However in some insulators there is an added effect due to the trapping of the thermalized irradiation electrons resulting in a net internal charge buildup. Under certain conditions it is possible for the charge buildup to initiate a spontaneous discharge. This effect has been noted in polyethylene terephthalate films when irradiated with a beta source.[1] It is the purpose of this work to identify the trapping of irradiation electrons and to characterize the thermal release from traps.

The primary effects due to any irradiation of polyethylene terephthalate are induced changes in the electrical properties, structural damage and chemical changes resulting in the evolution of gases. Some of these effects are obviously correlated, however these correlations are either unknown or not well understood although many of these changes have been investigated and are well documented.[2,3,4] In any attempt to understand charge storage and thermal release of electrons one must ultimately depend upon fundamental material properties. Therefore, it is necessary to understand the irradiation effects associated with charge transport, space charge buildup and related phenomena observed in various materials.

Radiation induced conductivity and space charge regions have been investigated in related materials. Yahgi[5] has found a gamma-ray induced conductivity for polyethylene and polytetrafluoroethylene. The relationship between induced current and dose rate is explained in terms of electron trapping and recombination statistics. In diamond the ionized electrons and holes become trapped at energy levels with sufficient lifetimes and densities to establish an appreciable space charge.[6,7] Adhern[8] has used alpha particle bombardment of diamond to establish an internal field corresponding to 480 volts per centimeter.

Although the above observations are for insulators with well defined crystalline regions, other insulating materials such as amorphous silica have yielded similar results. Pensak[9] reports on induced conductivity by electron bombardment in various insulating materials where the results can be interpreted as ionization and an internal space charge buildup due to trapping of the charge carriers. The effect is shown to be proportional to the amount of energy absorbed in the insulator from the electron irradiation.

Murphy[10] has observed polarization of dielectrics by electron irradiation. Occasional spontaneous discharges have been noted. The observed phenomenon cannot be interpreted in terms of macroscopic electrical properties such as volume resistivity or dielectric constant but seems to be related to charge storage capacity due to existing traps or radiation induced traps with sufficient density and at deep enough levels to permit regions of space charge to exist for extended periods of time at room temperature. Polytetrafluoroethylene was studied, and

the charge storage effect noted; however, definite conclusions are lacking.

Gross[11,12,13] has reported on numerous irradiation effects in solids. Borosilicate glass and plexiglass approximately 1 cm in thickness were bombarded with 2 mev electrons and the space charge distribution and discharge were investigated. In certain instances the space charge was released using a pointed electrode in contact with the irradiated sample. The high field near the point initiated a discharge. Charge release measurements using thermal activation of the stored charge were also reported. The space charge distributions were qualitatively described by the irradiation electrons located in a narrow layer near an effective range and a positive compensation charge located near the unirradiated surface.

The work of Fowler[14] provides the most direct information about the trapping of electrons in polyethylene terephthalate where the analysis is based upon the energy band theory of solids. Studying x-ray induced conductivity an electron trap density greater than 10^{17} traps/cm^3 was determined. Also the decay time for the induced conductivity of various materials was measured and subsequently related to the thermal release of electrons from traps and recombination. For the observed behavior, Fowler was able to quantitatively explain the results by assuming either a uniform or an exponential distribution of traps in depth measured by the number per cubic centimeter per electron volt referenced to the conduction band. In a rather broad classification the uniform distribution corresponded to the amorphous materials while the exponential distribution was associated with polycrystalline

material. It was suggested that the exponential distribution is associated with the boundaries between the crystalline regions.

The results obtained about space charge buildup in electret-forming materials must also be considered. The electret and persistent internal polarization have received extensive treatment in the literature.[15,16] Murphy,[17] et al., have investigated the phenomena in the presence of penetrating beta rays. As a result of the investigation, a tentative model for the formation of persistent polarization has been proposed. Molecular ionization, electron diffusion over microscopic distances in an applied field and freezing of the electrons in deep traps is used to describe the sequence of events yielding the space charge regions.

Although the cited references are pertinent to the description of electron trapping and thermal release there are additional factors of interest to the behavior of capacitor-type structures in a beta environment. The space charge buildup results in an internal electric field. It has been noted that this field can initiate a spontaneous discharge.[1,10] To obtain more insight into the occurrence of the discharge events, it is necessary to obtain more detailed information about the trapping of irradiation electrons. For this purpose a capacitor-type structure shown in Figure 2.1 has been irradiated with electrons from an electron gun. An electron beam with insufficient energy to penetrate the structure was used to inject electrons which become thermalized and are subjected to the conductive mechanisms of the polyethylene terephthalate. Trapping of these electrons results in a charge buildup. If the charge buildup does not initiate a spontaneous discharge, the decay of the space charge after irradiation has ceased can be observed under certain

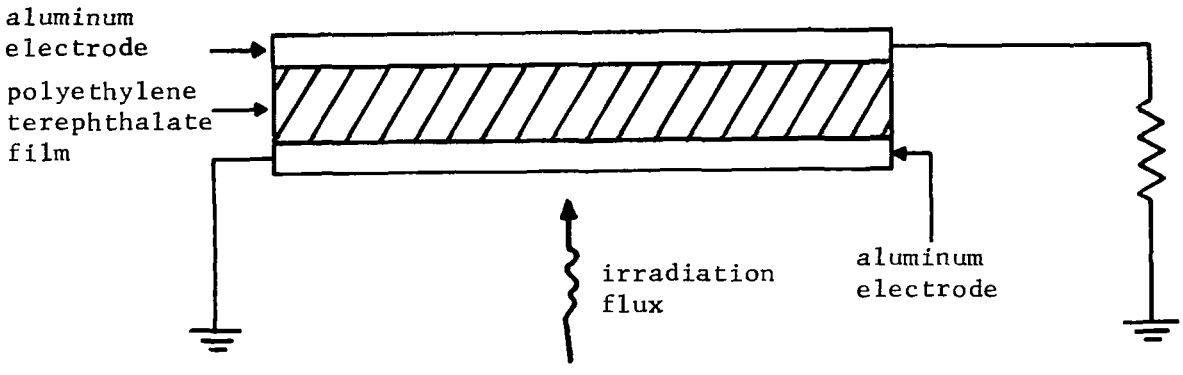

Figure 2.1. Capacitor-Type Structure with Polyethylene Terephthalate Dielectric and Evaporated Aluminum Electrodes.

conditions. These conditions are established by constructing a model for the transfer of external charge due to the space charge decay and for electron trapping and thermal release. Using this model to analyze the data one can infer the number of traps per cm^3, the trap distribution with respect to the number per cm^3 per electron volt of energy below the conduction band, the half-lifetime of the trapped electrons, and the dependence of the stored charge upon the energy of the primary electrons.

2.2 Experimental

The apparatus used to inject electrons into the polyethylene terephthalate films are shown schematically in Figure 2.2. The electron source is a heated tungsten filament. The electrons are accelerated through a potential supplied by a regulated dc supply. Electrostatic and magnetic focusing are provided in the gun housing in conjunction with a deflection system. The irradiation chamber is a glass assembly with three ports. In addition to providing a mount for the gun assembly, one port is attached to an oil diffusion pump and the other port used for mounting the polyethylene terephthalate films. The power supply has a ripple of less than 0.5 percent RMS with an output voltage resolution of 2 percent. The electron gun can be stabilized over a voltage range from 10,000 volts to 50,000 volts for currents in the range from 1 nanoampere to 1 milliampere. The diameter of the beam can be focused to one centimeter at the irradiated surface. Pressure in the working chamber measured at the diffusion pump port is maintained below 10^{-5} torr during all irradiations.

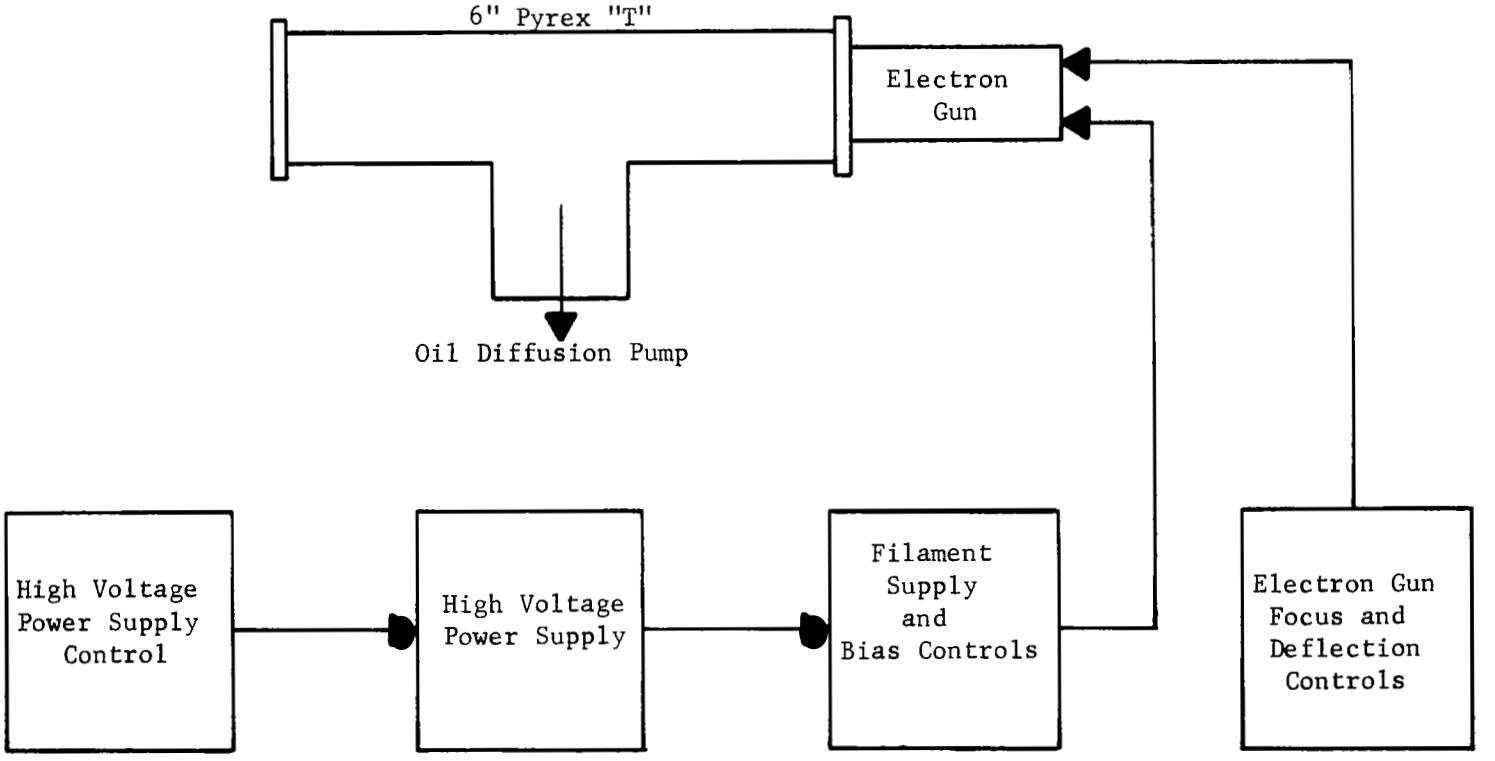

Figure 2.2. Schematic Representation of Electron Gun Assembly.

The samples are mounted on the fixture shown in Figure 2.3. This arrangement was employed after it was found that insulators in the system must be eliminated to obtain reproducible results with respect to charge storage in polyethylene terephthalate. The films are held in place by magnets. The irradiated electrode makes electrical contact with the steel plate which is system ground and the contact to the back electrode is provided by the magnet which is in electrical contact through bare copper wire with a vacuum feed-through in the mounting plate. The aluminum front plate provides a shield against the electrons outside the irradiation area and specifically at the sample edges while the lead provides attenuation for any bremsstrahlung created in the aluminum. A shutter is used to position the beam and to measure the beam current. ZnS suspended in collodium is used as a phosphor coating on the aluminum shutter and provides visual alignment and focusing. To obtain reproducible areas over the energy range of interest an aluminum foil (2.54×10^{-3} cm thick) with a 1 centimeter diameter hole was positioned between the electron gun and the shutter. The foil is electrically connected to the electron gun so that any irradiation electrons stopped by the foil will not be detected in the metering circuit. Using a slightly defocused beam, the current density determined by the phosphor glow was more uniform than for a focused beam alone. The beam current was measured by rotating the shutter so the electron beam is striking the aluminum portion of the shutter and by passing the collected electrons through a meter to the high voltage power supply. In the energy range from 10 kev to 50 kev, backscattered electrons are approximately 15 percent of the primary beam current.[18] The secondary

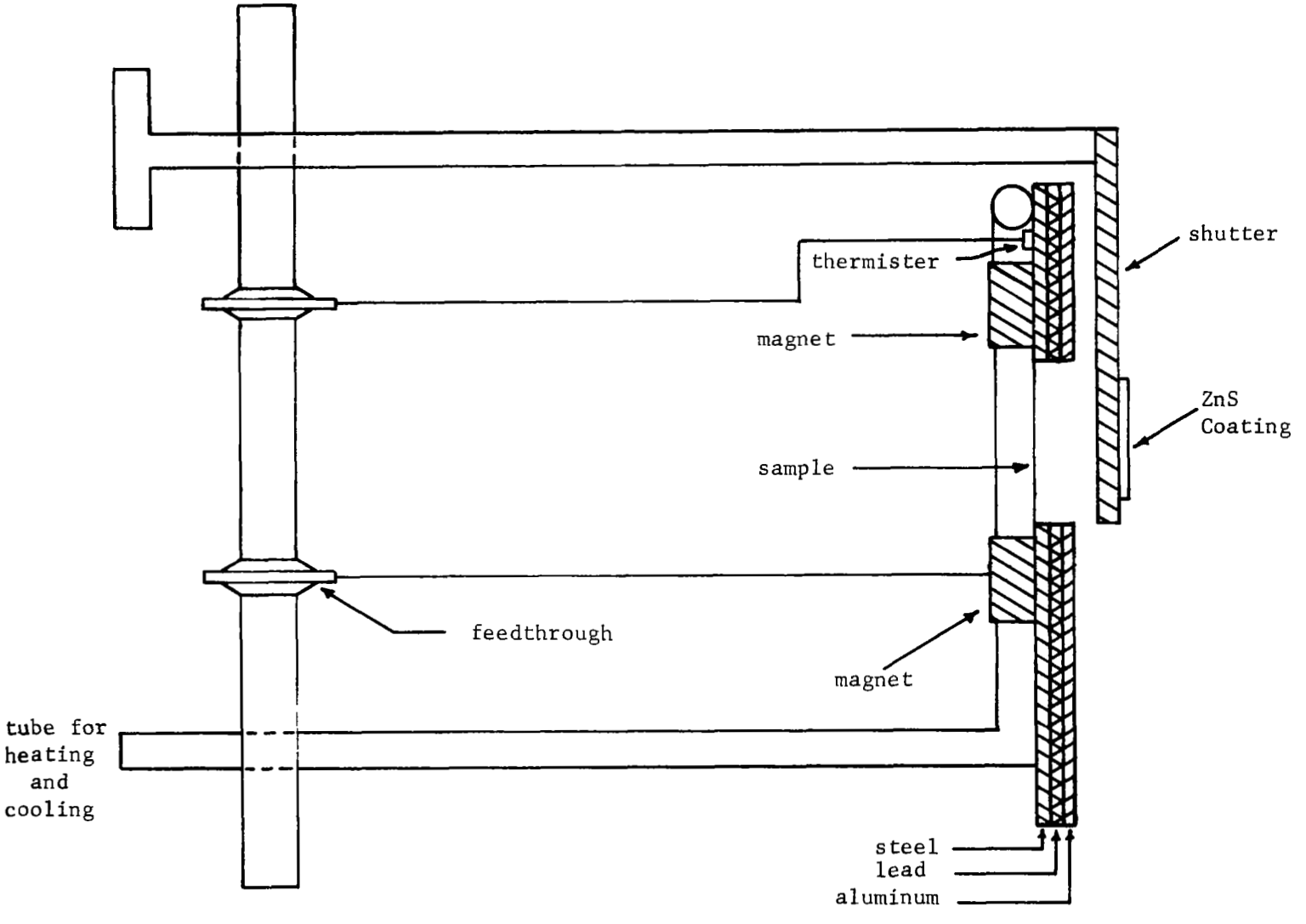

Figure 2.3. Fixture for Mounting Sample in Electron Gun Assembly.

yield is approximately the same value.[19] Therefore, the current measured by this technique can be in error as much as 30 percent with respect to the current actually striking the shutter. When the shutter is removed the electron beam is incident on the aluminum electrode of the test sample. The secondary electrons from the irradiated surface will be approximately the same as for the shutter, however the backscattered electrons will depend upon the thickness of the aluminum electrode.[19] Since the backscattering coefficient is smaller for aluminum films of interest approximately 1000 Å thick than for bulk aluminum, the number of primary electrons which are able to provide secondary electrons at the aluminum-polyethylene terephthalate boundary or which are able to penetrate into the polyethylene terephthalate will be larger than the value measured by the shutter current. The error involved is estimated to be approximately 20 percent. For the data to be presented, this error is not important. Only when one attempts to estimate the efficiency for charge storage, which is the number of irradiation electrons trapped with respect to the number of primary electrons, will this measurement need be considered in detail.

Provisions for cooling and heating the sample were included. However the inability to provide uniform heating or cooling of a suspended film limited the value of any data other than at ambient temperature. It was estimated that variations as much as 30°C could exist across the sample parallel to the electrodes.

The irradiated samples were prepared from commercially available polyethylene terephthalate.[20] Films 6.3×10^{-4} cm thick and 5 cm in diameter were cleaned twice in a detergent solution and rinsed after

each wash in deionized water. Following a wash in hydrofluoric acid, and a deionized water rinse, the films were stored in methanol prior to electrode evaporation. After placing the films in the evaporator, and outgassing for approximately 30 minutes, aluminum electrodes were evaporated to the desired thickness.

After evaporating the electrodes, the sample was placed in the system as shown in Figure 2.3. The capacitance and dissipation factor were measured at 1 kc with typical values of 6 nanofarads and 0.005 respectively. The dc leakage resistance was measured with values greater than 10^{12} ohms acceptable. The reason for this requirement will become evident after discussing the detection of space charge decay.

As discussed in Appendix A, asymmetrical decay of the trapped electrons will result in a transfer of charge through an external circuit. The circuit used to detect this charge is shown in Figure 2.4. The RC network integrates the current in the external circuit with a time constant of 10^5 seconds. The voltage across the capacitor is measured by an electrometer whose input resistance is a portion of the RC integrator. The output of the electrometer is fed into a strip-chart recorder running at a speed of 2.54 cm per minute. The minimum voltage across C_1 which can be measured is 1 millivolt.

After placing the sample in the irradiation chamber, an electron beam with a current density of 5×10^{-8} amperes/cm^2 was focused on the shutter. The shutter was then opened for the desired irradiation time. The energy of the electrons for each irradiation was in the range from 10 kev to 20 kev. Upon terminating the irradiation, the electrodes of

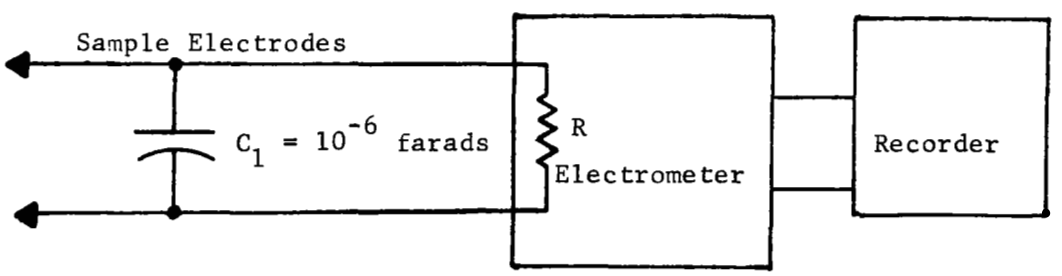

Figure 2.4. Circuit used to Measure External Charge Transfer Resulting from Thermal Release of Trapped Electrons.

the sample were shorted for a period of one minute. This allows any transients due to turning off the electron beam to decay and provides ample time to connect the measuring circuit shown in Figure 2.4 across the sample. Due to the high impedance levels encountered in the measurement it was impractical to achieve the transition from the electron beam measurement to the trapped charge decay measurement with a switching device. The trapped charge decay was observed from 60 seconds to approximately 2400 seconds after turning off the electron beam. The transfer of external charge as a function of time under these conditions is shown in Figure 2.5 for a typical sample. From this data alone it would be difficult to identify the trap distribution. However one aspect of the external charge transfer is quite obvious. Using range-energy data for water[21] which is approximately the same as that for polyethylene terephthalate one readily finds that the range of the primary electrons at the energy which yields the maximum external charge transfer is approximately one-half the thickness of the polyethylene terephthalate film. Also the energy at which the external charge transfer is reduced below the sensitivity of the measurement corresponds to a practical range approximately equal to the film thickness. For the latter observation one may conclude that within the sensitivity of the measurement the trapped-charge decay is symmetrical. The simplest trapped charge distribution which could yield such a result is one that is uniform throughout the irradiated volume. Obviously there are other distributions which could yield a symmetrical decay; however, when one considers the transmission of electrons in this energy range through comparable thicknesses of other materials the linear decrease in the number of

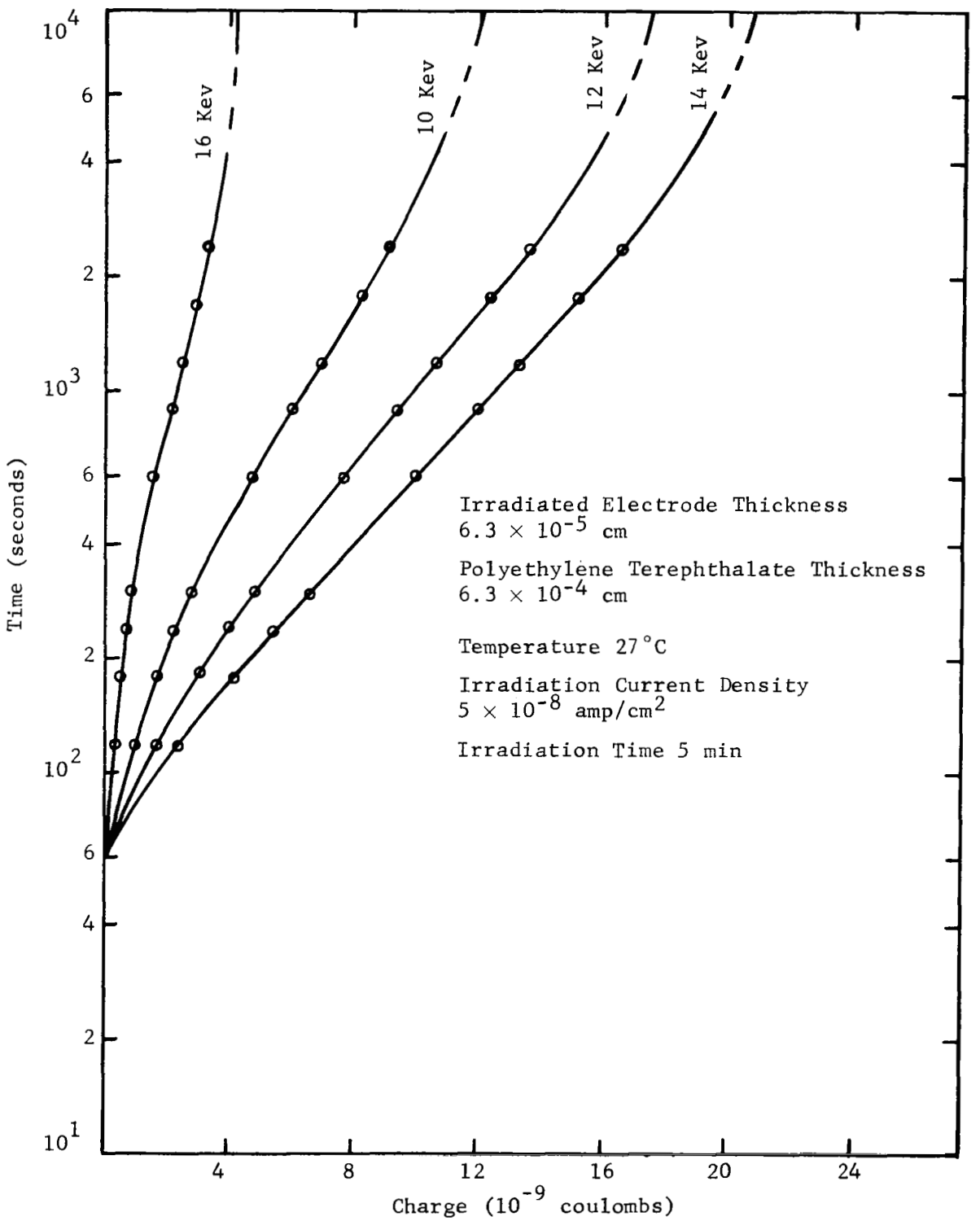

Figure 2.5. External Charge Transfer from Thermal Release of Trapped Irradiation Electrons for the Indicated Primary Electron Energies.

electrons with depth is a reasonable assumption.[22] In general, one finds a somewhat less than linear decrease near the irradiated surface. The possibility of secondaries from the electrode being injected into the polyethylene terephthalate could increase the number of electrons trapped near the irradiated surface such that the overall distribution is more uniform than one might expect based upon the transmission of primary electrons alone.

The contribution of secondary electrons from the irradiated electrode to the net charge distribution in the polyethylene terephthalate film was further identified by the results shown in Figure 2.6. A sample was prepared in the usual manner with 500 Å electrodes and irradiated with 16 kev electrons. The beam current density was 5×10^{-8} amperes/cm^2. After observing the trapped charge decay the irradiated electrode thickness was increased to 1000 Å, 2000 Å, 5000 Å, 7000 Å, and 10,000 Å and the sample irradiated with 16 kev electrons and a beam current density of 5×10^{-8} ampere/cm^2 at each thickness. The measurement was repeated at each thickness and the reproducibility was well within the sensitivity of the measuring technique. The results indicate that while the number of primaries entering the polyethylene terephthalate is decreasing due to the increased aluminum electrode thickness, the transfer of external charge initially increases and subsequently decreases with increasing electrode thickness. This initial increase can be explained in terms of the secondary yield from the exit side of the irradiated aluminum electrode. This secondary yield has been correlated with the energy dissipation density at the exit surface.[19] For electrons in the energy range of interest the

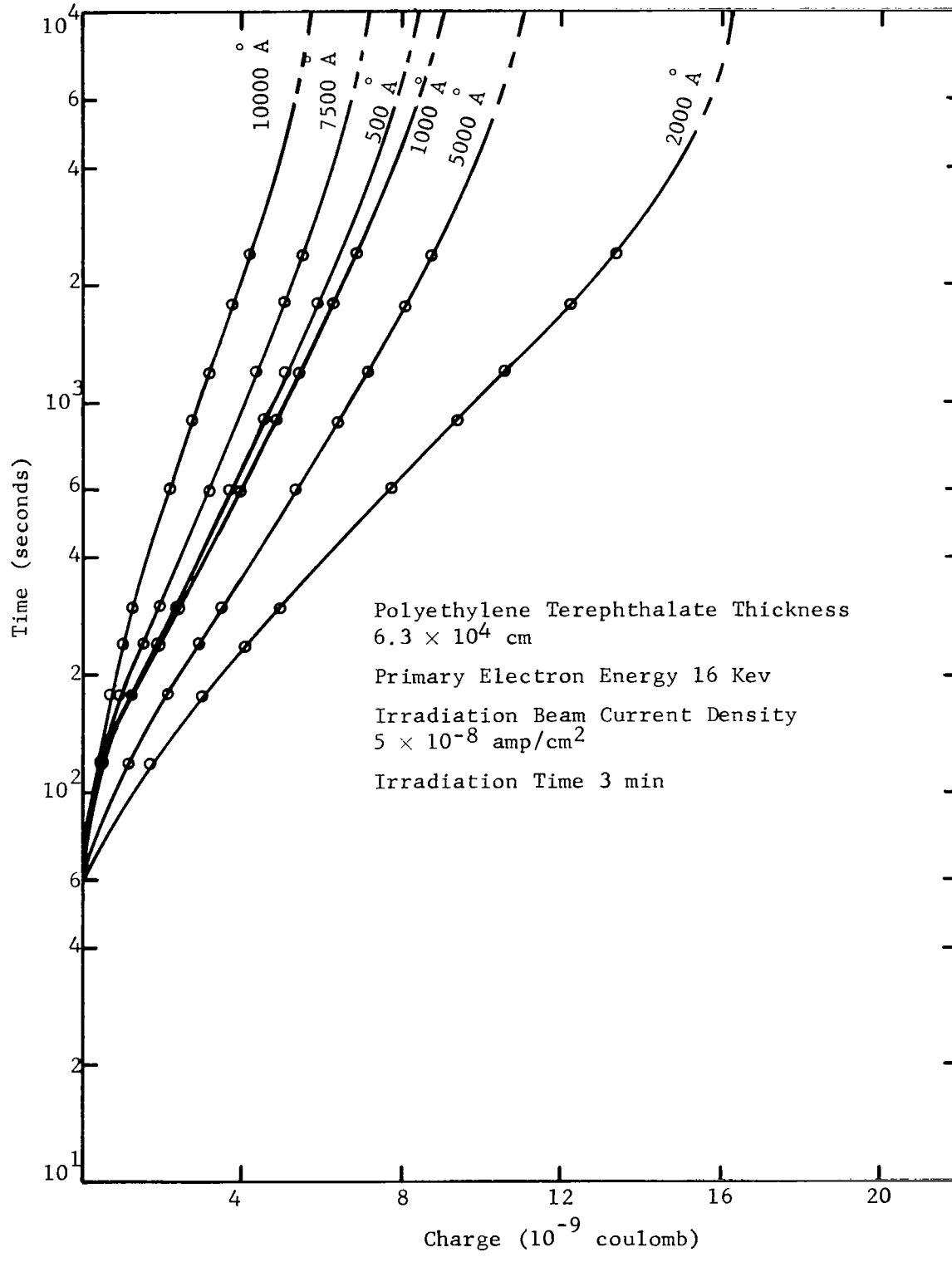

Figure 2.6. External Charge Transfer as a Function of Time for Irradiated Aluminum Electrode Thickness Indicated.

energy dissipation function in aluminum has a maximum at approximately one-fourth the practical range of the primary electron.[23] For a 16 kev electron in aluminum this maximum occurs at approximately 7000 Å. The increased secondary yield is at the expense of the number of primary electrons transmitted through the aluminum electrode; therefore, the electrode thickness which will yield the maximum number of electrons injected into the polyethylene terephthalate will be less than or equal to 7000 Å depending upon the rate of increase in the number of secondaries and the rate of decrease of the number of primaries with increasing electrode thickness. Other factors which can affect the net charge distribution are the secondary electron yield from the irradiated polyethylene and the diffused energy spectra of the electron beam transmitted through the electrode. These effects would decrease the external charge transfer with increasing electrode thickness. Therefore, the results of Figure 2.6 are consistent with the expected behavior when one considers the net charge in the polyethylene terephthalate due to primary and secondary electrons.

The dependence of the external charge transfer on the energy of the primary electron in Figure 2.5 can now be interpreted in terms of the practical range corresponding to the various energies and the change in the number of primary and secondary electrons injected into the polyethylene terephthalate. To indicate this dependency consider the net charge distribution to be uniform from the irradiated surface to the practical range. Furthermore, for primary electron energies less than the energy corresponding to the maximum transfer of external charge, assume that all the electrons thermally released from traps arrive at

the irradiated electrode without being retrapped. Under these conditions, Equation (A.13) can be used to relate the limiting value of the external charge transfer. Since all the surface charge on the unirradiated electrode must be transferred through the external circuit,

$$Q_{ext}(max) = \frac{q\bar{n}_t v_1 d_1}{d} \tag{2.1}$$

where v_1 is the irradiated volume and d_1 corresponds to the practical range of the primary electrons. The product $\bar{n}_t v_1$ represents the net charge which is a function of the primary electron range. It is not possible for the present analysis to apply Equation (2.1) to the results in Figure 2.6. The main difficulty is with the product $\bar{n}_t v_1$ and its relationship to the primary electron energy. A qualitative description has been given which is consistent with the results, however, a detailed analysis will not be attempted. Another difficulty associated with Equation (2.1) is the assumption that all electrons thermally released from traps arrive at the irradiated electrode without being retrapped. Since the trapped charge distribution extends through approximately one-half the thickness of the polyethylene terephthalate for the maximum external charge transfer, some of the thermally released electrons should reach the unirradiated electrode. Therefore, any analysis which equates the maximum value of external charge transfer to the surface charge on the unirradiated electrode will predict a minimum value of trapped charge.

External charge transfer during the thermal release of trapped electrons can be used to obtain quantitative information if one restricts the observations to a single energy thereby keeping the irradiated volume and practical range constant. In this manner, the number of trapped

electrons within a given irradiated volume can be varied using a series of irradiation times at a fixed beam current. The same result could in general be obtained by keeping the irradiation time fixed and varying the beam current. However for the present work the possibility of a saturation effect for the trapping and thermal release of irradiation electrons made the former approach more attractive. The primary electron energy was 14 kev with a beam current density of 5×10^{-8} ampere/cm^2. Irradiation time was varied from 30 seconds to 30 minutes and the results are shown in Figure 2.7.

Using the analysis of the uniform trap density with energy measured from the conduction levels as described in Appendix B and assuming that the most likely occurrence involving the electrons thermally released from traps is drift to an electrode resulting in partial neutralization of the space charge, a minimum value for the number of trapped electrons, for the trap density and for the half-lifetime in traps can be determined. This explicitly assumes that recombination involving ionized hole-electron pairs and retrapping in the space charge region are second order effects during the space charge decay. From the work of Fowler,[14] one suspects that recombination is less likely than retrapping. Therefore, a necessary condition for the stated assumptions to be reasonable is that the mean range traveled toward the irradiated electrode by a thermally released electron be comparable to the practical range of the primary irradiation electrons. This results in the expression $\left|E\right|_{max}\tau\mu \sim 10^{-4}$ cm where $\left|E\right|_{max}$ is the maximum value of the internal field, τ is the lifetime of the free carrier when multiple trapping occurs and μ is the drift mobility of the carrier. The value of $\left|E\right|_{max}$ is used to obtain the order of magnitude

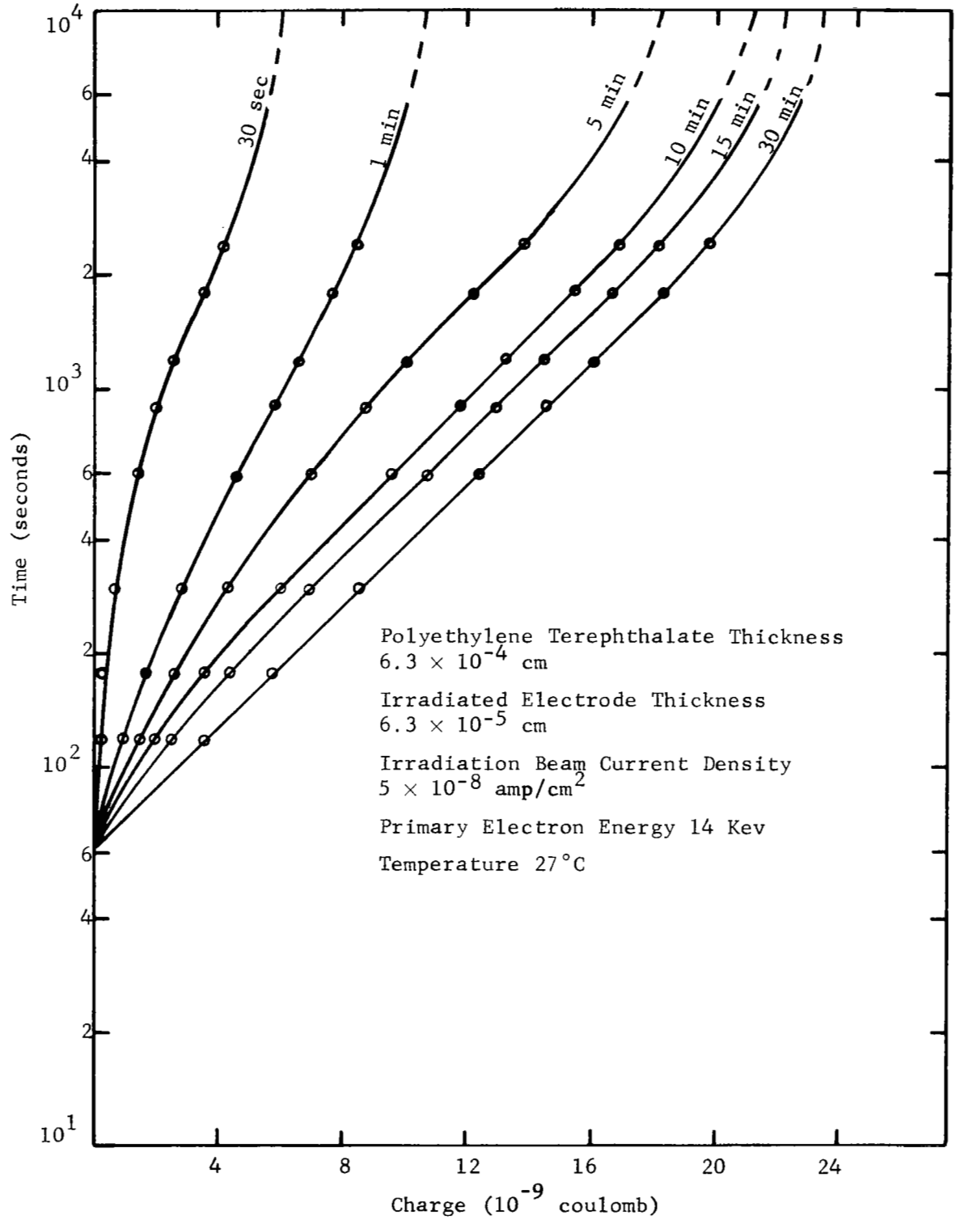

Figure 2.7. External Charge Transfer as a Function of Time for the Indicated Irradiation Period.

for the internal field throughout most of the space charge region. From the present work it will not be possible to substantiate this expression, however the phenomenological descriptions in Appendix B derived from the simple no-retrapping model are adequate to explain the observations in Figure 2.7. From Figure 2.7 the saturation effect is deduced from the manner in which the released charge as a function of time approaches the limiting solution in Figure B-2. As the irradiation time is increased, there is not a corresponding increase in the external charge transfer. From dark conductivity measurements an average value for the equilibrium Fermi-level of $E_{fo} \sim 0.9$ ev has been determined. Therefore the $\gamma \geq 10^4$ curve in Figure B-2 and Equation (B.13) can be used to approximate the number of trapped electrons per cm^3 at t = 0 where

$$n_t(0) \simeq 0.23 \frac{B}{kT_c} . \tag{2.2}$$

The value of $\frac{B}{kT_c}$ can be obtained from the slope of the limiting solution in Figure 2.7. Considering Equation (B.21)

$$\frac{dn_r(t)}{dt} = \frac{BkT}{kT_c} . \tag{2.3}$$

To relate the minimum number of electrons in traps to the measured external charge transfer for 14 kev primary electrons, Equation (2.1) can be used where $d_1 \simeq \frac{d}{2}$ and $v_1 = A_1 d_1 \simeq d_1$ cm^3. Therefore

$$\bar{n}_t \simeq \frac{8Q_{ext}(max)}{qd} . \tag{2.4}$$

Scaling the results in Figure 2.7 to reflect the asymmetry considerations of Equation (2.4) yields $\frac{B}{kT_c} = 1.7 \times 10^{16}$ per cm^3 per electron volt.

Therefore, the minimum value of trapped electron density for the limiting value is 4.25×10^{15} electrons/cm^3.

For the assumption of uniform net charge density from the irradiated surface to the practical range of the primary electrons (d_1), Equation (2.4) can be used in conjunction with Poisson's equation to obtain a lower limit for the internal electric field at the irradiated surface of the polyethylene terephthalate film. Using the values $d_1 = 3 \times 10^{-4}$ cm, $d = 6 \times 10^{-4}$ cm, $q = 1.6 \times 10^{-19}$ coulomb, $Q_{ext}(max) \simeq 20 \times 10^{-9}$ coulombs, $\epsilon = 2.83 \times 10^{-13}$ farad/cm in Equation (A.11) yields $\left|E\right|_{x=0} = 1.9 \times 10^5$ volts/cm. Furthermore if one assums that $n_t = \bar{n}_t$, the internal electric field at t = 0 for the limiting value in Figure 2.7 is $\left|E(x = 0,\ t = 0)\right| = 5 \times 10^5$ volt/cm. It has been possible to gain some confidence in these values of internal electric field using an applied voltage and observing the current flow before irradiation, during irradiation and after irradiation. With no bias applied, the current flow after irradiation has ceased is in a direction such that the irradiated electrode is negative with respect to the unirradiated electrode. An external dc bias was applied to the polyethylene terephthalate capacitor in a manner to oppose the current flow due to space charge decay. At various bias levels, the capacitor was irradiated with 14 kev electrons for 15 minutes at a current density of 5×10^{-8} amps/cm^2. For a bias less than 350 volts the current flow immediately after irradiation ceased was in the direction consistent with space charge decay to the irradiated electrode for zero bias. After approximately 10^3 seconds the current flow was in a direction consistent with the applied dc bias. However for a bias greater than 350 volts the current flow was in the

direction determined by the applied bias. For the 6×10^{-4} cm polyethylene terephthalate the applied electric field necessary to overcome the space charge effect is approximately 5.6×10^{5} volts/cm for the 15 minute irradiation.

One further aspect of the thermal release of trapped electrons can be obtained from this analysis. The minimum time required for half the trapped electrons to be released can be obtained for the limiting value in Figure 2.7 using Equations (B.14) and (B.20) where

$$\frac{n_t(x,0)}{2} = \frac{B}{2kT_c}\left[E_{fo} - E_{fn}(x)\right] = Bm[-0.5 - \ell n\, a\alpha] \quad . \qquad (2.5)$$

Using the values obtained in the present analysis yields a value of 48 seconds. It was found during the course of these experiments that the reproducibility for a given sample was within the sensitivity of the measurement if charge release was observed for a time in excess of 10^3 seconds. Since residual charging effects which would effect the reproducibility were not noted, this value of half-lifetime seems reasonable. It is also worth noting that the upper limit for application of Equation (B.20) where $t \leq \frac{0.1}{s\alpha}$ was calculated to be 1.1×10^3 seconds. Although the upturning characteristics in Figure 2.7 have been added through theoretical considerations, this behavior has been observed for times in excess of 5×10^3 seconds. However for integration times approaching 10^4 seconds the error involved is comparable to the deviation resulting in the upturning portion of the curve.

2.3 Discussion

Trapping of irradiation electrons in polyethylene terephthalate films has been investigated and results obtained which are consistent

with a simple no-retrapping thermal release model. A limiting value for irradiation electron trapping has been identified. The trap density as a function of energy was found to be uniformly distributed with a value of 1.5×10^{16} cm^{-3}. This is in contrast to Fowler's work[14] where the distribution was exponential with a density of 10^{20} cm^{-3}. The results of the present work cannot provide detailed information about this difference however there are certain aspects which offer an explanation. Fowler concludes that 10^{20} cm^{-3} trap density appears too large and chooses the value which represented the extent to which the traps were filled by ionizing radiation. The more reliable value was quoted as 10^{17} cm^{-3}. This compares more favorably with the present work. Also, one must recognize that the quasi-Fermi level for the limiting value of irradiation electron trapping was only 0.23 ev from the equilibrium Fermi level while the induced conductivity resulted in 0.3 to 0.5 ev excursion of the quasi Fermi level. Therefore one might argue that over the region of interest the trap density is more uniform than for those where the traps are filled closer to the conduction band. In fact, Fowler hints to observations which indicate that the deeper traps are relatively more numerous than expected from the exponential distribution.

The reproducibility for the measurement of trapped irradiation electron decay provides additional information about two aspects of the present work. In general the reproducibility of the limiting value for thermal release of trapped irradiation electrons from sample to sample was poor. However, the results for each sample were qualitatively consistent with those presented for a typical sample. The reproducibility

of the charge release measurement for repeated irradiations of a given sample depended upon the number of times the particular sample had been irradiated. For the initial irradiations on a newly prepared sample, charge release measurements were not consistent with the measurements obtained from subsequent irradiations. However, after the initial irradiations, the reproducibility of the charge release measurements were within the sensitivity of the measuring technique. This dependence suggests that the trapping sites are radiation induced. From the present work it is not possible to substantiate this concept. The reproducibility of trapped irradiation electron decay also suggests that the residual charge buildup is negligible for the present work. The half-lifetime of trapped charge and the deviation toward a limiting value in Figure B-2 are consistent with this observation. Under continuous irradiation there appears to be a limiting value of trapped charge as shown by the results in Figure 2.7.

Another aspect of the present work which requires additional comment is the asymmetry considerations developed in Appendix A which are used to obtain quantitative information from the charge release measurements. Although one can certainly argue that the assumption of total charge release to the irradiated electrode is not realistic, it is obvious that this concept will predict minimum values for the model. In certain instances these minimum values can be used as an approximation to the actual values. One instance where this approximation seems reasonable requires that (1) the practical range of the primary irradiation electrons is only a small fraction of the sample thickness, (2) the probability of thermally released electrons in the space charge region

extending from the zero field point to the irradiated surface reaching the irradiated electrode without being retrapped is much greater than the probability of the thermally released electrons in the space charge region extending from the zero field point to the practical range reaching the unirradiated electrode without being retrapped. For those cases where the practical range of the irradiation electrons is comparable to the thickness of the samples, a difference in the trapping cross section for thermally released electrons on either side of the zero field point will determine the asymmetry of space charge decay. If no retrapping occurs from the zero field point to the irradiated electrode while multiple trapping occurs from the practical range to the unirradiated electrode represents a reasonable assumption. For the present work this concept is best described by the dependence of trapping cross section upon the extent to which the traps are filled in the various regions of the sample. However as the practical range increases such that the probabilities in (2) become comparable, the asymmetry considerations developed in Appendix A becomes unreasonable. The agreement cited in the present work between the calculated value of internal electric field resulting from trapped irradiation electrons and the applied electric field required to overcome this effect indicates that the minimum values obtained from the charge released measurements can be used as an approximation to the actual values.

Chapter III

Space Charge Buildup and Spontaneous Discharge

3.1 Introduction

Trapping of irradiation electrons in insulating materials has been substantiated experimentally.[10,11] In view of earlier work,[14] one might expect considerable charge buildup to occur in electron irradiated polyethylene terephthalate. To achieve a large irradiation electron density in traps, fast electrons are injected into polyethylene terephthalate which reach thermal velocity through scattering and ionization. For practical considerations, evaporated aluminum electrodes cover the surfaces of the polytheylene terephthalate. The interaction of the primary irradiation electrons with the electrode material must be considered to identify the injected electrons. For the present analysis it will be assumed that the injected electrons become thermalized uniformly throughout the volume determined by the cross sectional area and the practical range of the primary electron beam. Experimental evidence related to this assumption has been considered in Chapter II. As a result of this assumption one can proceed in a straightforward manner to determine the internal electric field for a given number of trapped irradiation electrons. In addition the detection of external charge transfer associated with spontaneous discharge initiated by the internal field can be discussed.

The observations of spontaneous discharge have been obtained using a ^{147}Pm beta source for irradiation. The beta source was chosen for a very practical reason. The differential flux is an approximation to the Van Allen belt over the energies of interest. The current applications

of polymers in space technology derives special interest from this experiment. Irradiation for extended periods is possible with this approach without concern for stabilizing the energy and flux rate.

3.2 Internal Electric Field

To calculate the internal electric field resulting from trapped irradiation electrons consider the simple model in Figure 3.1 where the diameter of the irradiated area A_1 is much greater than the thickness d. Electrons are injected at x = 0, uniformly across the area A_1. It is assumed that all of these electrons are stopped within a distance d_1 in the polyethylene terephthalate and result in a uniform charge density ρ for $x < d_1$ and charge density zero for $x > d_1$. Therefore by Poisson's equation

$$\nabla^2 V = -\frac{\rho}{\epsilon} \qquad 0 \leq x < d_1 \tag{3.1}$$

$$\nabla^2 V = 0 \qquad d_1 < x \leq d \quad . \tag{3.2}$$

Using the boundary conditions that the potential is zero at the extreme boundaries

$$V(0) = V(d) = 0$$

and that the displacement vector is continuous across the boundary at $x = d_1$, the electric field in these two regions is

$$E = -\frac{qn_t}{\epsilon}\left[x - \frac{d_1}{d}\left(d - \frac{d_1}{2}\right)\right] \qquad 0 \leq x \leq d_1 \tag{3.3}$$

$$E = -\frac{qn_t d_1^2}{2\epsilon d} \qquad d_1 \leq x \leq d \tag{3.4}$$

The results of Equations (3.3) and (3.4) are shown in Figure 3.2.

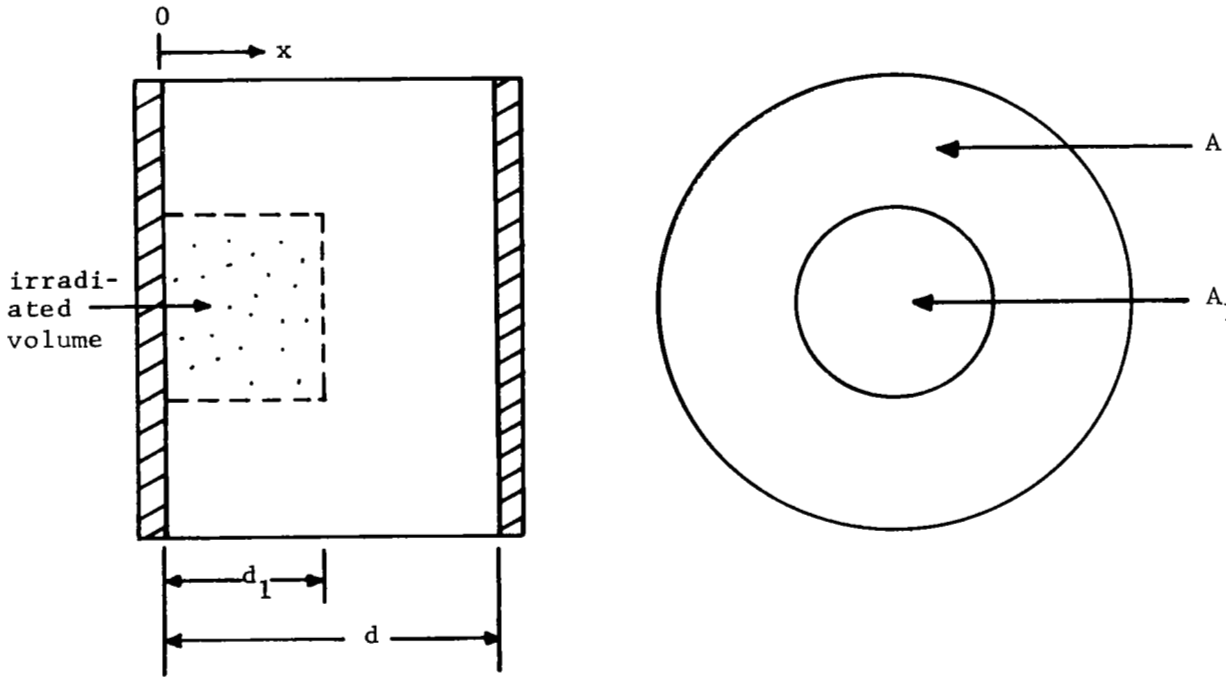

Figure 3.1. Geometry of Sample and Irradiated Volume Assumed to Yield a Uniform Charge Distribution Throughout the Volume $A_1 d_1$.

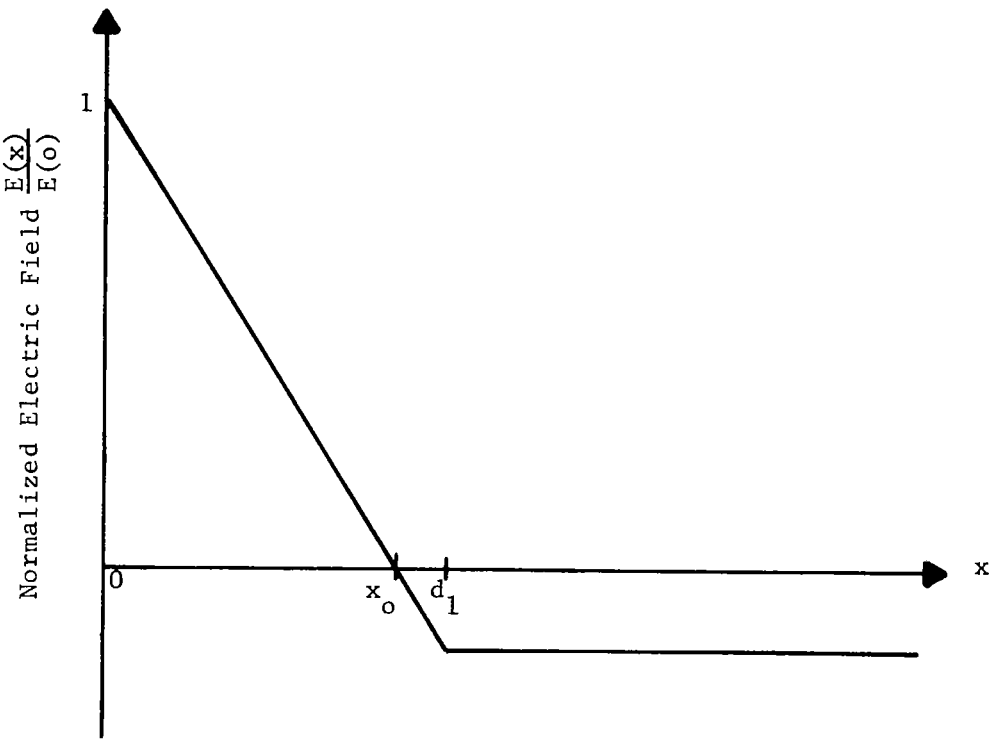

Figure 3.2. Electric Field Distribution Resulting from Uniform Charge Distribution Density for $x \leq d_1$ and zero for $x \geq d_1$.

For breakdown due to the internal electric field only the value of $|E_{max}|$ will be considered. For $d_1 < d$ the maximum electric field occurs at $x = 0$. Also if $d_1 \ll d$

$$|E_{max}| = |E(0)| \simeq \frac{qn_t d_1}{\epsilon} . \tag{3.5}$$

Therefore the number of electrons per cm^2 (n_{A_1}) in the volume $A_1 d_1$ required to yield a given value of E_{max} is

$$n_{A_1} = \frac{\epsilon |E_{max}|}{q} . \tag{3.6}$$

If $d_1 = d$ which requires that the charge be distributed uniformly throughout the entire volume ($A_1 d$), the maximum electric field occurs

at x = 0 and x = d and is

$$\left|E_{max}\right| = \frac{qn_t d}{2\epsilon} \quad . \tag{3.7}$$

Again the electrons per cm^2 required to yield a given value of $\left|E_{max}\right|$ can be determined by

$$n_{A_1} = \frac{2\epsilon \left|E_{max}\right|}{q} \quad . \tag{3.8}$$

The results of Equations (3.6) and (3.8) are shown in Figure 3.3. Clearly the value of $\left|E_{max}\right|$ differs only by a factor of 2 as d_1 goes from $d_1 \ll d$ to $d_1 = d$ for a given number of electrons per cm^2 (n_{A_1}) in the region of charge density. Therefore the remainder of the analysis will consider only the case where charge is distributed uniformly through the entire volume ($A_1 d$).

Due to the presence of an internal field resulting from a net trapped charge, field induced breakdown can occur. The breakdown mechanism could be either Zener or electron avalanche. The Zener breakdown depends upon the change in rate at which electrons pass from the valence band to the conduction band under the action of a constant electric field. Avalanche breakdown results when free electrons are accelerated by the constant electric field and gain more energy from the field than is given up through lattice collisions. Thus the electron is able to obtain enough energy to cause ionization and secondary electrons which result in an avalanche process. Generally it is thought that collision ionization by electrons is responsible for breakdown of solid dielectrics.[24] Quoted values for the field strength (electric field required to initiate breakdown) for polyethylene terephthalate range from 2×10^6 volts/cm

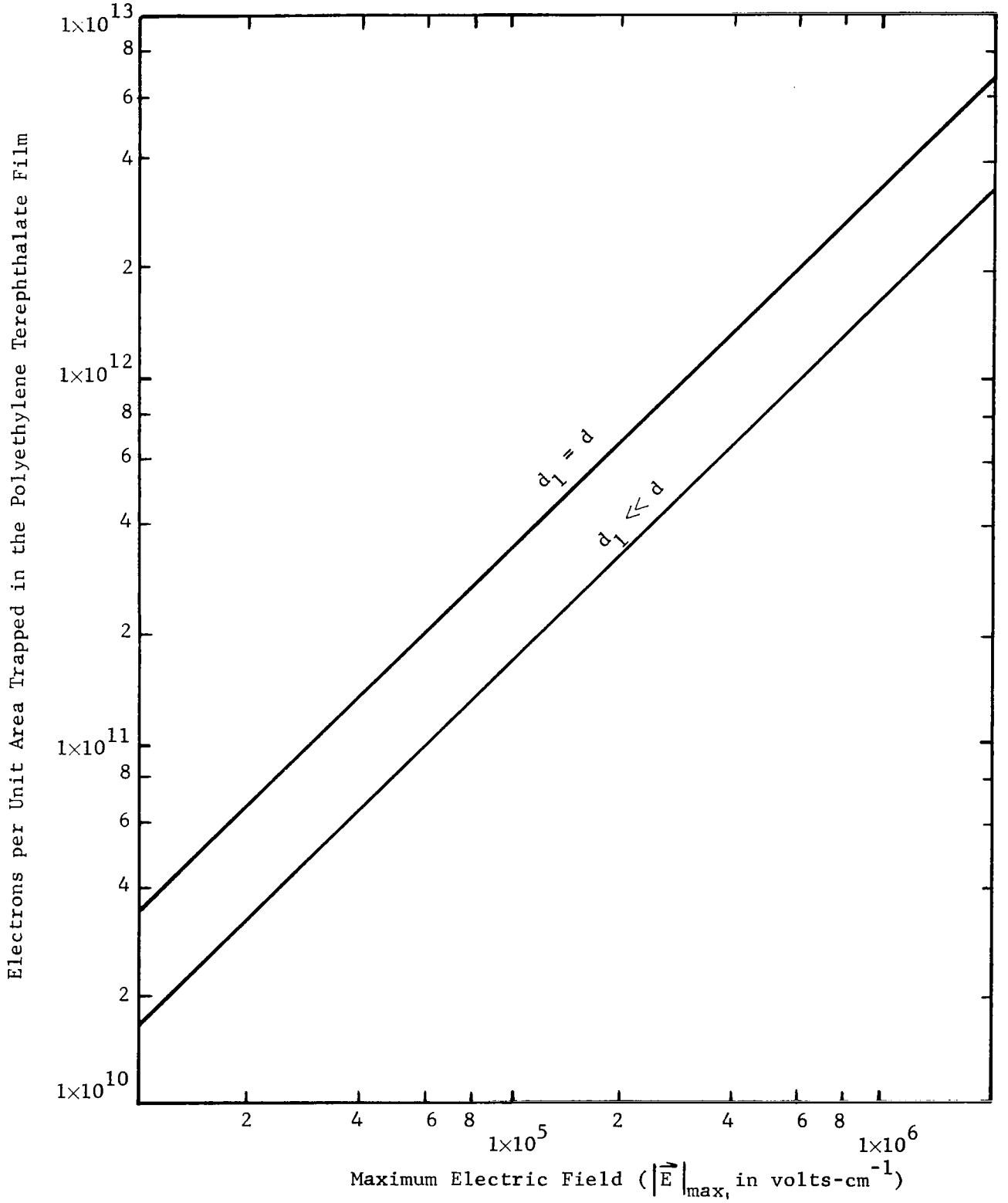

Fig. 3.3. Maximum Built-in Field for a Uniform Electron Density.

to 6×10^6 volts/cm.[25,26] These values are nearly independent of: (a) voltage transient in the range 10^{-6} to 10^3 sec, (b) temperatures ranging from -180 to 25°C, and (c) thickness in the range of 5 to 6×10^{-4} cm.[25] Often breakdown pulses are observed for much lower fields than those stated above. In fact Inuishi[25] has found that the most probable breakdown process at room temperature with thin films or large electrodes areas is failure at a defect. This is due to the localization of the electric field at a defect center where charge trapping occurs and to lattice irregularities which reduce the intrinsic field strength of the material.

Field strength of polyethylene terephthalate has been shown to be sensitive to irradiation. After irradiating a 5×10^{-3} cm sample with a dose of 10^7 rads of 2 Mev electrons at a dose rate of 10^6 rads/min the breakdown field strength decreased by 10 percent.[26] This decrease is also a function of dose rate with the most pronounced change occurring at the lower dose rates.

Assuming a uniform density of trapped charge through the polyethylene terephthalate, breakdown will be initiated either where the electric field is a maximum or at a localized defect where the electric field at the defect exceeds the breakdown field strength of the region. The breakdown initiated at defects will depend upon the nature and location of the defect.

3.3 External Charge Transfer from Spontaneous Discharge

The breakdown mechanism has been discussed to this point without concern for detecting the occurrence of the trapped charge liberation. The transient across the load resistor in Figure 3.4 can be analyzed

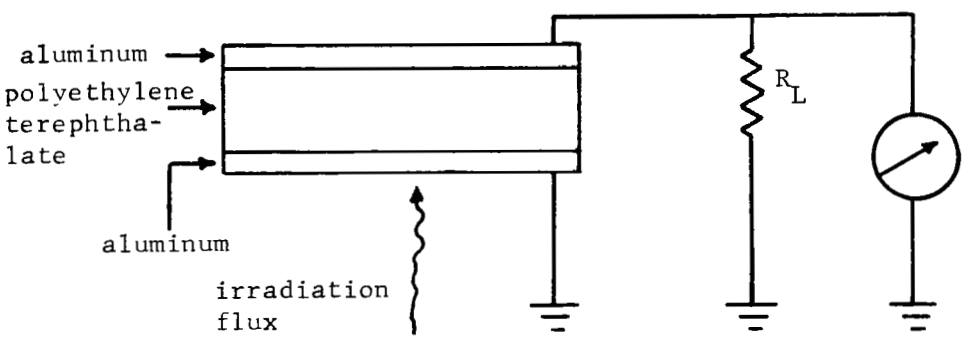

Figure 3.4 Simplified Circuit for Detecting External Transfer of Charge from Spontaneous Discharge.

by calculating the external charge transfer resulting from spontaneous discharge. When $|E_{max}|$ is large enough to initiate breakdown at the surface, the value of charge liberated can range from the total charge in traps to only an infinitesimal volume of charge in the region about a defect. For localized breakdown the amount of charge liberated is probably confined to the region near the defect since the remainder of the dielectric is not subjected to either the localized field or the reduced intrinsic strength associated with the defect. Therefore it is expected that defect breakdown may be approximated by assuming a variable field strength and a subsequent volume of charge liberated. To do this consider Figure 3.5 where only a portion of the sensor is irradiated and breakdown occurs in a volume less than or equal to the irradiated volume. In addition, assuming that the maximum extension of the discharge region parallel to the electrodes is greater than the thickness of the polyethylene terephthalate will greatly simplify the calculations. This assumption permits one to consider the various regions of the structure independently.

If breakdown occurs to electrode number 2 and removes a volume $A_2 d_2$ of trapped electrons in Figure 3.5, one can calculate the surface charge density over the area A_2 on electrode 1 before and after breakdown using Equation (3.3). If the liberated charge is assumed to be liberated and recombines at electrode number 2 in zero time, the difference between the values of surface charge density over area A_2 before and after breakdown on electrode number 1 represents the charge which must be transferred from electrode 1 to electrode 2 through the load resistor R_L to reach an equilibrium state of charge distribution. Since the displacement vector component D_x is continuous across the boundary at x = 0 the magnitude of the surface charge density over A_2 before breakdown (σ_B) on electrode 1 is

$$\sigma_B = \left| D_x(0)_B \right| = \epsilon \left| E_{max_B} \right| = \frac{qn_t d}{2} \quad . \tag{3.9}$$

For the stated assumptions the magnitude of the surface charge density over A_2 after breakdown (σ_A) at electrode 1 is

$$\sigma_A = \left| D_x(0)_A \right| = \epsilon \left| E_{max_A} \right| = qn_t \left[\frac{d_1}{d} \left(d - \frac{d_1}{2} \right) \right] . \tag{3.10}$$

Therefore the net surface charge which must be transferred from electrode 1 to electrode 2 is

$$\sigma_s = \sigma_B - \sigma_A = \frac{qn_t}{2} - \frac{qn_t d_1}{d} \left(d - \frac{d_1}{2} \right)$$

$$= \frac{qn_{A_2}}{2} - \frac{qn_{A_2}}{d} \left(d - \frac{d_1}{2} \right) . \tag{3.11}$$

The polyethylene terephthalate structure with electrodes constitutes a capacitor and at the time t = 0+ the voltage due to the net surface

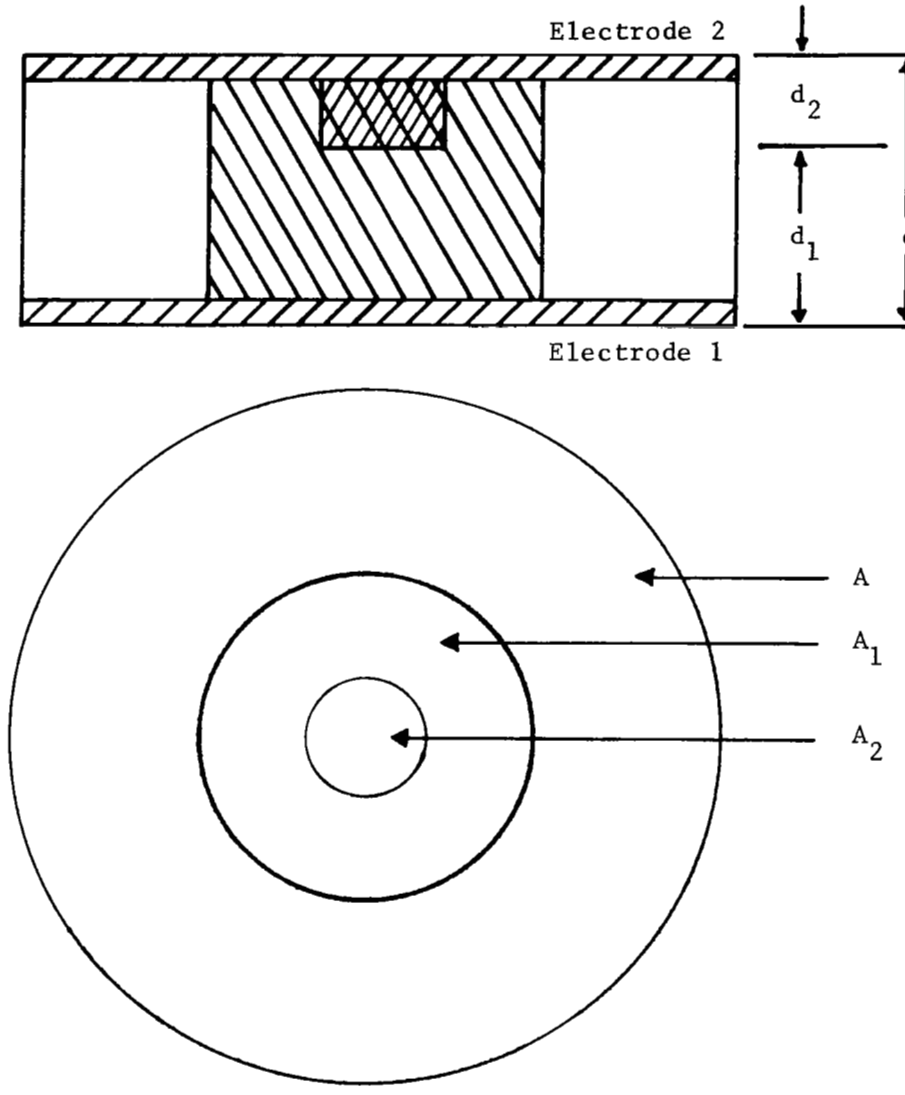

d = thickness of capacitor
d_2 = depth of discharge
A = area of capacitor
A_1 = area of irradiation
A_2 = area of discharge

Fig. 3.5. Assumed Geometry for Irradiation Resulting in Uniform Charge Trapping Throughout Volume $A_1 d$ and Discharge Throughout Volume $A_2 d_2$.

charge can be found from

$$\sigma_s = \frac{Q}{A_2} = \frac{C}{A_2} V \tag{3.12}$$

or

$$\left|V_c(0)\right| = \frac{qn_{A_2} A_2 d_2}{2C_A Ad} = \frac{qn_{A_2} v_2}{2C_A v_c} \tag{3.13}$$

where v_2 is the discharge volume and v_c is the capacitor volume. This voltage also appears across R_L and a characteristic RC discharge transient results where

$$V = V_c(0)\, e^{-t/R_L C} . \tag{3.14}$$

To evaluate the magnitude of the voltage at t = 0+ one must know the value of electrons/cm^3 in traps and the volume of charge liberated. For defect breakdown, assigning values to these quantities would be meaningless. However, after calculating the magnitude of voltage associated with breakdown initiated by $\left|E_{max}\right|$ an upper limit for defect breakdown can be established. Using the value of $\left|E_{max}\right| = 10^6$ v/cm the corresponding charge in traps under the assumptions used to develop Equation (3.8) would be 3.4×10^{12} electrons/cm^2. For 6.3×10^{-4} cm thickness of polyethylene terephthalate the capacitance is 4.18×10^{-10} farad/cm^2. Thus

$$V_o = 650 \frac{v_2}{v_c} \text{ volts} . \tag{3.15}$$

For defect breakdown occurring under the stated assumptions the discharge transient is directly related to the volume of charge liberated.

3.4 ^{147}Pm Experiment

Obtaining the expected performance of electrical components and devices in a space radiation environment requires a technique for simulating this environment. Those devices primarily affected by electron irradiation are usually tested by Van de Graeff accelerator bombardments. This work describes the design, construction, and results of radioisotope source of ^{147}Pm used in electron irradiation studies. It is believed that such a source will be quite useful in further studies of this kind.[27]

The primary interest is in the charge storage effects in dielectric materials caused by the trapping of incident electrons trapped in the material and is relatively insensitive to the spacial distribution of the trapped electrons. The maximum variation in the electric field produced is a factor of two when one considers the two extremes of homogeneous trapping and trapping entirely at one surface. For our studies an electron source with energies between 10 and 200 Kev is desirable. The source strength should be sufficient to give a flux of at least 10^9 electrons per square centimeter per second at a distance of 2 centimeters from the source.

Considerations of availability, cost, emitter energy spectrum and half-life suggested the use of ^{147}Pm as a possible source. It is available in large quantities, inexpensive, is a pure beta particle emitter with a maximum energy of 223 Kev, and has a half-life of 2.6 years. Calculations indicated that a 70 curie ^{147}Pm source would provide the desired characteristics if: (1) it could be deposited to a thickness of 25 mg/cm^2 or less, (2) it could be deposited within an area of 25 cm^2, and (3) it could be used with a covering window of 5 mg/cm^2 or less. Such a source has been designed and constructed.

The ^{147}Pm source was constructed by first mixing promethium oxide powder homogeneously with potassium silicate powder and slurried in alcohol. This mixture was distributed evenly on the surface of a thin disc (0.3 cm thick by 5 cm in diameter) of magnesium silicate. After drying the disc was fired at 1100°C for 16 hours to react the promethium oxide with the silicate fluxing agent. Subsequently a 3.8×10^{-3} cm Pyrex glass overlay was fixed on the surface of the source by heating at 900°C to serve as a protective cover. The glass overlay covers only the center of the source, exposing about 0.6 cm of the rare earth glass source at the perimeter. It is believed that the source can be used quite safely in a controlled experimental program in which routine smear testing is performed on a frequent basis.

The finished source was estimated by the supplier to have a flux of electrons above 25 Kev of less than 4.6×10^{10} electrons per square centimeter per second at a distance of 2 centimeters. Figure 3.6 is an energy spectrum of the source that was taken with an anthracene crystal. A counting rate of about 3.4×10^{5} counts per minute was obtained by placing a 1 cm thick lead collimator with a 0.05 cm hole in it on top of the source. The source has a maximum energy of 175 Kev and has a maximum number of electrons at 75 Kev. The source output measured with a thin shell ionization chamber was 1000 r/hr at 7.5 cm from the surface. Distribution uniformity of the ^{147}Pm activity over the surface of the disc was determined by autoradiography using Polaroid film and shown in Figure 3.7. Current measurements using a Faraday cup are included in Appendix C.

The advantages of the ^{147}Pm source for electron irradiation studies are: (1) the radioisotope source is much cheaper in original cost and

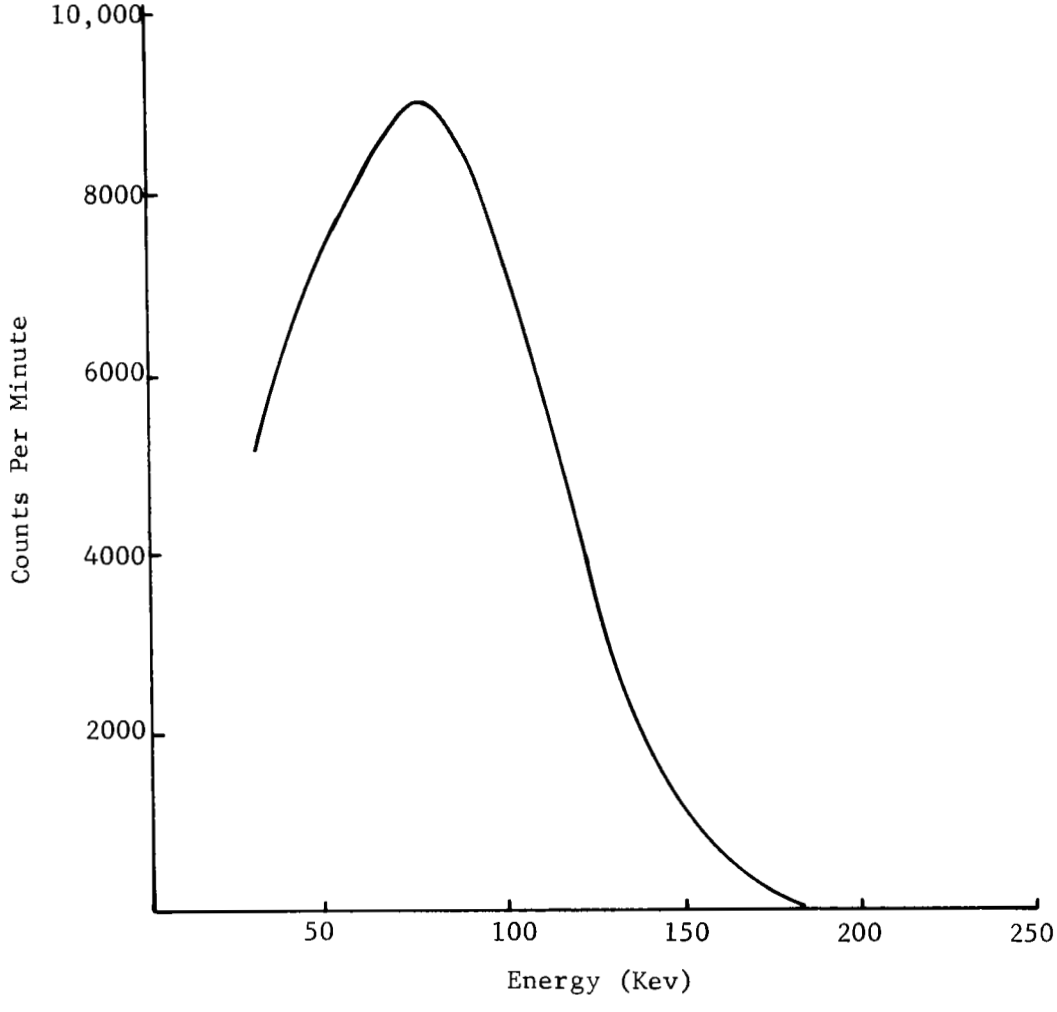

Fig. 3.6. Energy Spectrum of ^{147}Pm Source.

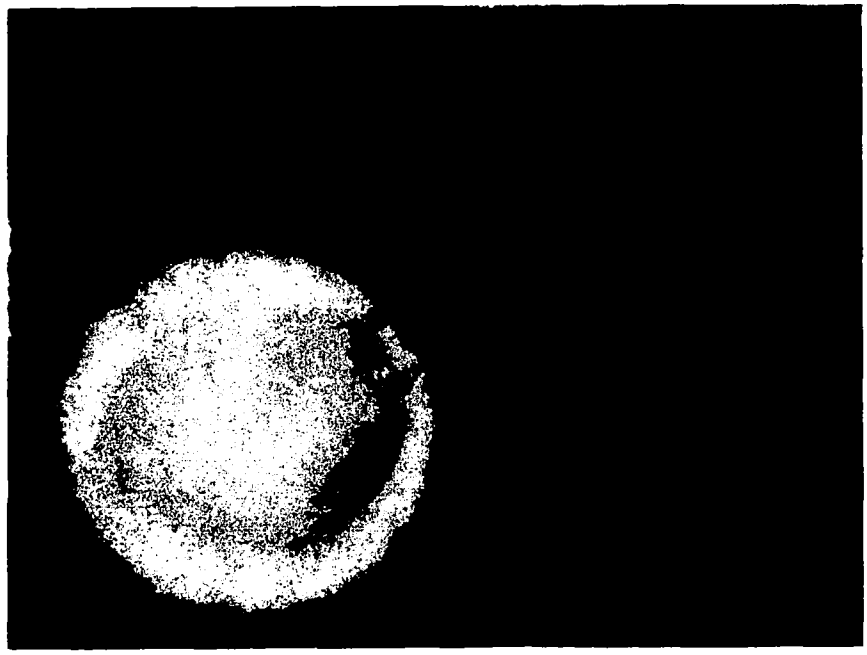

Fig. 3.7. Autoradiograph Using Polaroid Type 57 Film of ^{147}Pm Source for a 5 Second Direct Exposure.

operating expense than conventional machine sources, (2) the output of the source is constant and need be measured only once at known distances, (3) the irradiation time can be weeks or months, which is not practical with machine sources, and (4) the source can be used to simulate the electron distribution and frequency in space, thereby allowing more realistic "real time" testing programs.

The apparatus associated with the detection of spontaneous discharge are shown in Figure 3.8. The irradiation chamber is a glass assembly with two ports. One port is attached to an oil diffusion pump while the other is used for mounting the samples. The sample holder is similar to the one shown in Figure 2.3. The circuit used to detect the transfer of external charge resulting from a spontaneous discharge is shown in Figure 3.9. The sample was connected to the input of an electrometer. The input impedance of the electrometer and the capacitance of the sample determined the time constant of the discharge pulse. To provide continuous monitoring the electrometer output was connected to a strip chart recorder. The pass band of the recorder which is 200 cycles per second placed a limitation on the time constant of the pulse if minimum distortion of the pulse characteristics is desired. The capacitance of the sample was typically 22 nanofarads and the input impedance to the electrometer 10^7 ohms which results in a time constant of 0.22 seconds. The stray and lead capacitance was always less than 100 picofarads. The accuracy of the measuring circuit was determined using a capacitor about the same value as the sensors that were irradiated. The capacitor was charged with voltages from 0.002 to 0.100 volts and discharged through the input resistance of the electrometer using a mercury wetted relay. By adjusting

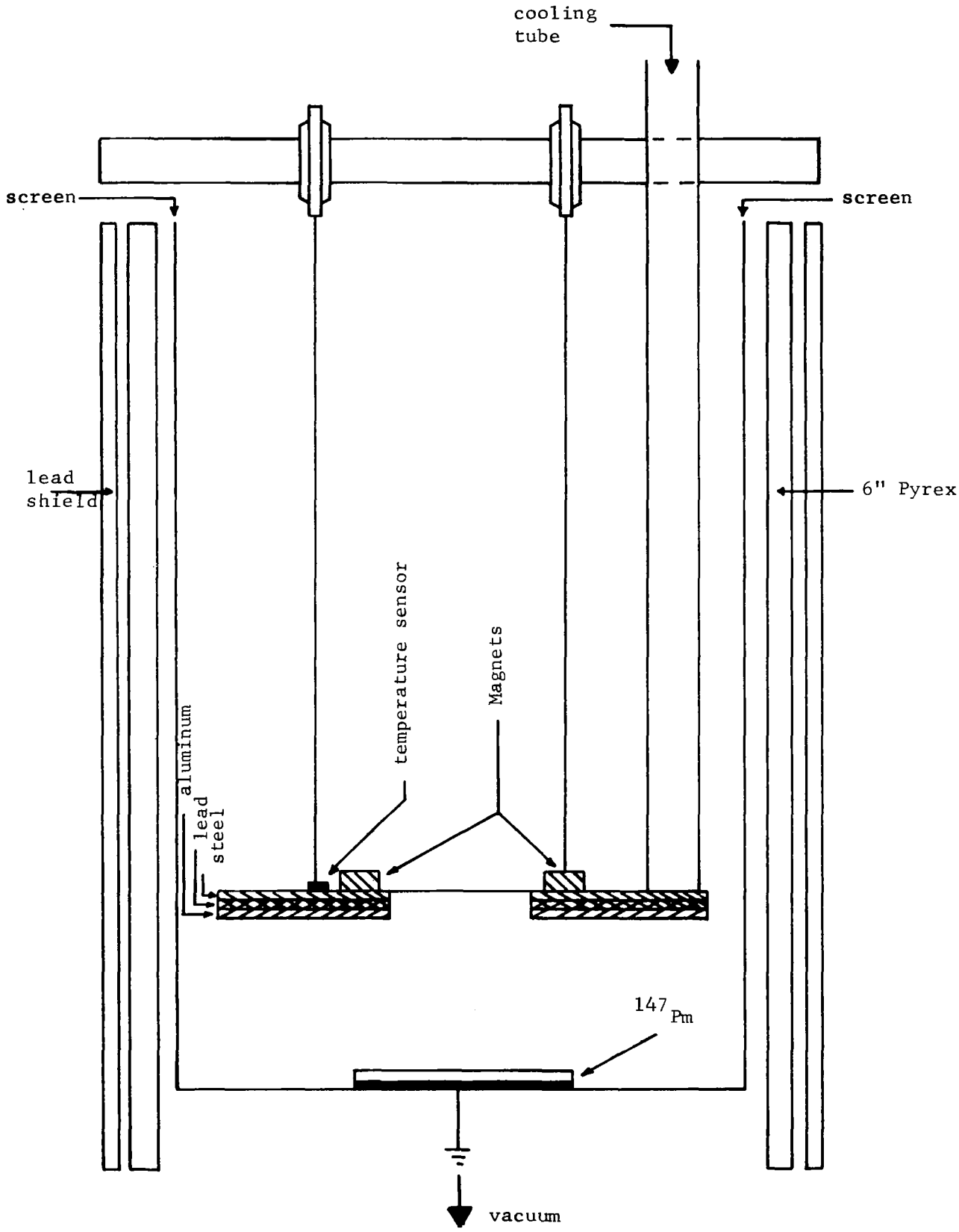

Fig. 3.8. Assembly for ^{147}Pm Experiment.

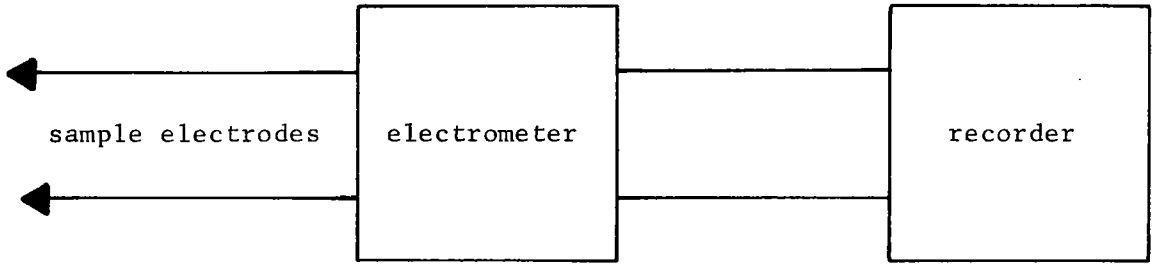

Figure 3.9. Block Diagram for Detecting Spontaneous Discharge.

the input resistance of the electrometer which is a portion of the RC circuit, different values of the decay time constant for the recorded pulses were obtained. Using these various time constants, the amplitude of the recorded pulses was compared to the initial voltage across the capacitor. The percent error observed for pulses less than 0.003 volt was less than 13.0 percent. An error of approximately 2 percent was measured for recorded pulses with amplitudes of 0.005 to 0.100 volts. The minimum pulse which could be measured was 0.001 volt. Therefore the characteristics of the discharge pulse should be obtained in the recorder output. This provides a discrimination technique whereby only those pulses with the proper decay time constant are counted. Other disturbances which may occur due to power line fluctuations, induction machinery start-up or other sources typically result in shorter time constants and can be disregarded. Disturbances of these sorts have been observed and correlated with the sources indicated.

Samples of 6.3×10^{-4} cm thick polyethylene terephthalate film with various thicknesses of aluminum electrodes with an area of 13 cm^2 were placed in the irradiation chamber approximately two centimeters from the

source. The flux rate was estimated to be 2.2×10^9 e/cm^2-sec by a current measurement as discussed in Appendix C. The irradiated area of the sample was 9.6 cm^2. The irradiated samples were connected to the circuit shown in Figure 3.9. Only those pulses with the proper time constant were counted as a discharge event. Very few spurious pulses, less than 1 percent of the total number of pulses observed, occurred during the observations. Due to the variations in types of samples irradiated and the difficulty in obtaining pulses a comprehensive evaluation of the ^{147}Pm experiment would be quite arbitrary. However, some aspects of spontaneous discharge for the conditions cited thus far in the report have been identified. For example there have been no pulses observed when the irradiated electrode of the sensor was 1 mil aluminum. Total irradiation time of these samples includes 648 hours at room temperature and 72 hours at -140°C.

For the 1/2 mil aluminum irradiated electrode, pulses have been observed at room temperature and -140°C. However only 2 samples out of the 5 tested have pulsed. For an irradiated electrode thickness of 0.025 mil, 6 out of the 16 irradiated samples pulsed. Throughout the ^{147}Pm experiment less than 50% of the samples irradiated have pulsed at all. Due to the difficulty in obtaining pulses, all the observations will be included as one statistic. Based upon an observed 668 pulses from 1/4 mil mylar dielectric with varying electrode thickness, the average pulse height was 72 millivolts with a maximum of 2.7 volts. The discrimination level was always in excess of 1 millivolt. The total irradiation time during which pulses were observed was 2754 hours. For an integrated flux of approximately 2.2×19^9 e/cm^2-sec, one obtains an

average value of 3.2×10^{13} e/cm^2-pulse. There seems to be no direct correlation between electrode thickness and pulse height nor an easily discernable correlation with pulse rate. This is not too surprising since the thickest foil used which has resulted in pulses, is 1/2 mil and this represents approximately one-half thickness for ^{147}Pm. For a total irradiation time of 402 hours on 5 samples with similar irradiation histories and similar geometries (0.025 mil irradiated electrode, 1/4 mil polyethylene terephthalate), 325 spontaneous discharges were recorded. The average pulse height was 30 millivolts. The average pulse rate for the total irradiation time of each sample was 0.57 pulses/hour. The average pulse rate after the first observed pulse was 8.6 pulses/hour. From these results two factors become apparent. The average external charge transfer due to spontaneous discharge is 6.6×10^{-10} coulombs. Also there is an initial buildup of trapped charge before the first spontaneous discharge. On the average the time interval between discharge events is at least an order of magnitude shorter than the irradiation time required to obtain the first pulse. This behavior is suggestive of partial discharge of trapped irradiation electrons as opposed to a discharge event where all trapped charge is liberated. With a capability to detect a one millivolt pulse, the distribution of pulse heights for one of the five samples is shown in Figure 3.10. The pulse heights are grouped by 5 millivolt intervals. The resulting distribution clearly shows that most of the pulses are less than the average value of 30 millivolts. In fact the distribution roughly approximates an exponential increase in the number of pulses as pulse height decreases. This wide variation is suggestive of the results of Equation (3.15) where the pulse height is related to the volume of discharge by

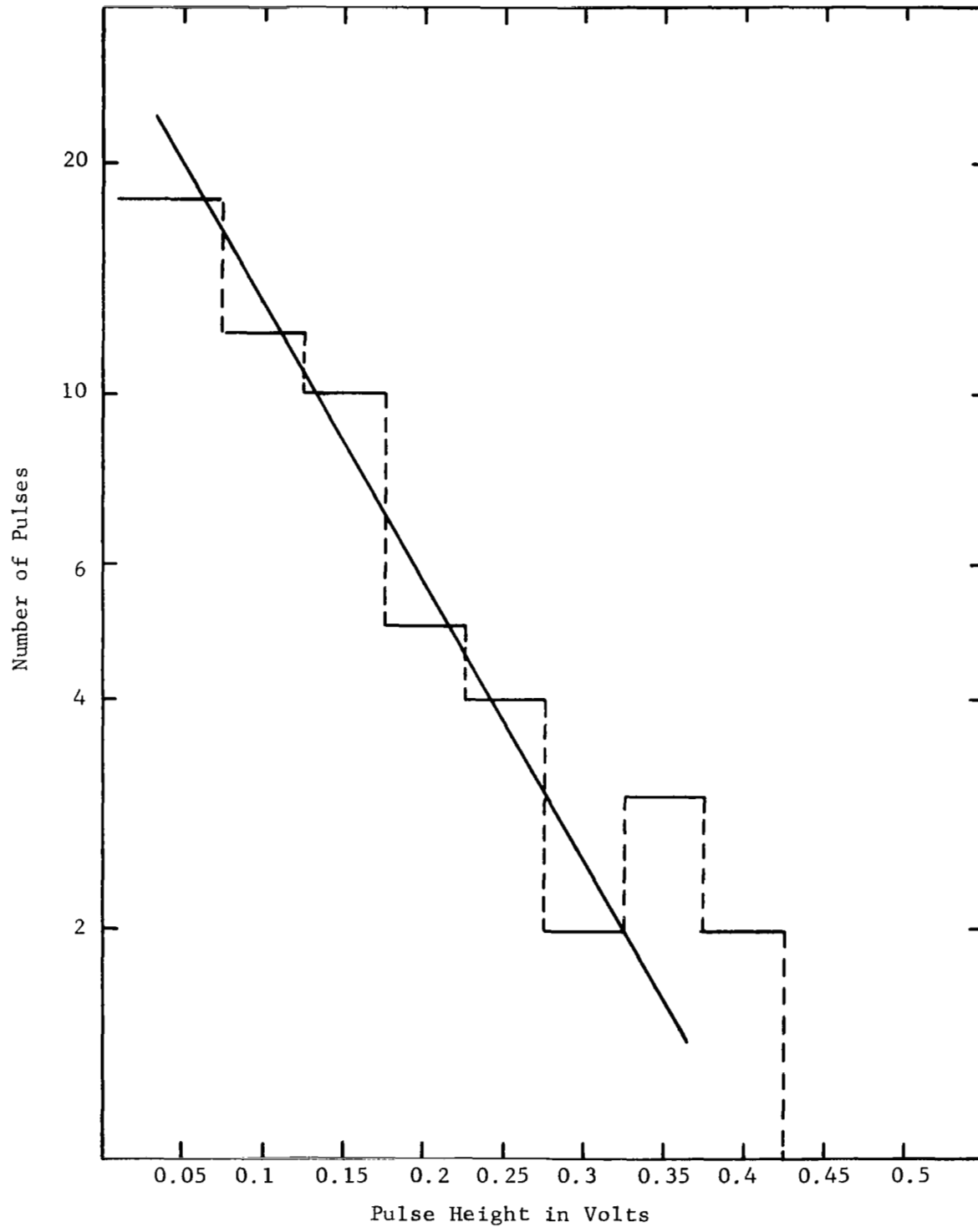

Fig. 3.10. Pulse Height Distribution from Spontaneous Discharge of Electron Irradiated Polyethylene Terephthalate Film.

$$V_o = 650 \frac{v_2}{v_c} \text{ volts} .$$

Based upon this concept the ratio $v_2/v_c = 4.6 \times 10^{-5}$ would represent the average volume of the sample involved in the discharge event.

Chapter IV

Related Experimental Observations

In addition to the observations of charge storage and release in polyethylene terephthalate at room temperature, other experiments related to the more general aspects of spontaneous discharge from electron irradiated insulating materials have been performed. The experiments fall into two major catagories: (1) observations related to the development of the charge storage and release model, and (2) observations of charge storage release in films other than polyethylene terephthalate. Observations related to the model include activation energy, dc field strength measurements, asymptotic behavior and low temperature charge release. Charge release measurements have been observed for polypropylene and cellulose acetate.

The activation energy measurements were made in a thermostated cell in a vacuum of 0.1 mm Hg. The main body of the cell was machined from brass stock and consists of two symmetrical pieces with an O-ring fitting to join the two sections under the force of a vacuum. Aluminum electrodes were evaporated onto each side of the films studied. The aluminum electrodes were contacted by optically polished metal electrodes held in place by small magnets. A guard ring was provided to limit the measurement to bulk properties. Teflon insulated coaxial connectors were used for electrical feed-throughs. The leakage resistance of the cell was greater than 5×10^{14} ohms at 30°C.

After mounting the sample in the cell and evacuating it, a 100 volt bias was applied through 10^{11} ohms input impedance to an electrometer. A typical current at room temperature for 1.0 mil polyethylene terephthalate with 100 volts applied bias was 4×10^{-12} amperes. The sample was

then heated at 1.25°C/min and the current and temperature recorded. Although thermal gradients obviously exist in the sample, it was estimated that the temperature as detected by a thermistor inside the cell was within 5°C of the actual temperature of the sample. This estimate was based upon a comparison between the monitoring thermistor and a thermocouple in contact with the sample.

From the dc conductivity vs 1/T plot shown in Figure 4-1, an activation energy for dark conductivity can be obtained. The data for polyethylene terephthalate have been average for four measurements. In addition a single measurement for polypropylene is shown in Figure 4-2. These data are important when the thermal release of charge is analyzed using the model developed in Chapter II.

The electric field strength of the dielectric was determined by placing the film between two optically polished metal electrodes and applying a dc voltage from a filtered power supply connected in series with the input impedance of an electrometer. The input impedance of the electrometer provided a current limiting resistance and a means for monitoring current fluctuations associated with breakdown. The applied voltage was increased in increments. Steady state current was obtained at each voltage level. When the voltage level was reached where large intermittent current fluctuations occurred without yielding a permanent short through the dielectric, the corresponding electric field was taken as a measure of breakdown which could best correlate with spontaneous discharge resulting from the trapping of irradiation electrons. For 1/4 mil polyethylene terephthalate, the intermittent current fluctuations occurred at an applied electric field of 6.6×10^5 v/cm. For

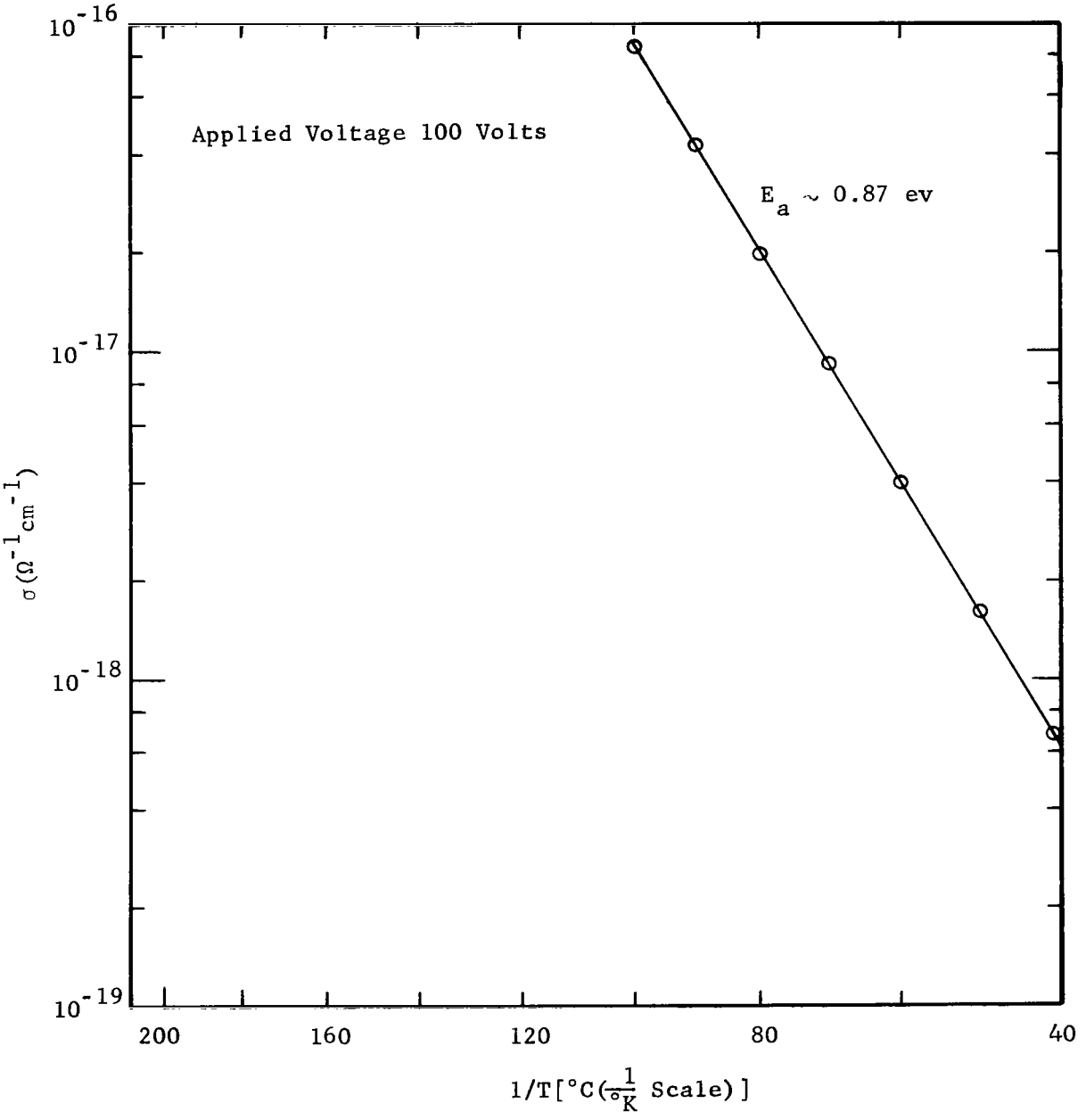

Figure 4.1. Conductivity vs 1/T for 1 mil Polyethylene Terephthalate Film (Data Points Represent Average of Four Independent Measurements).

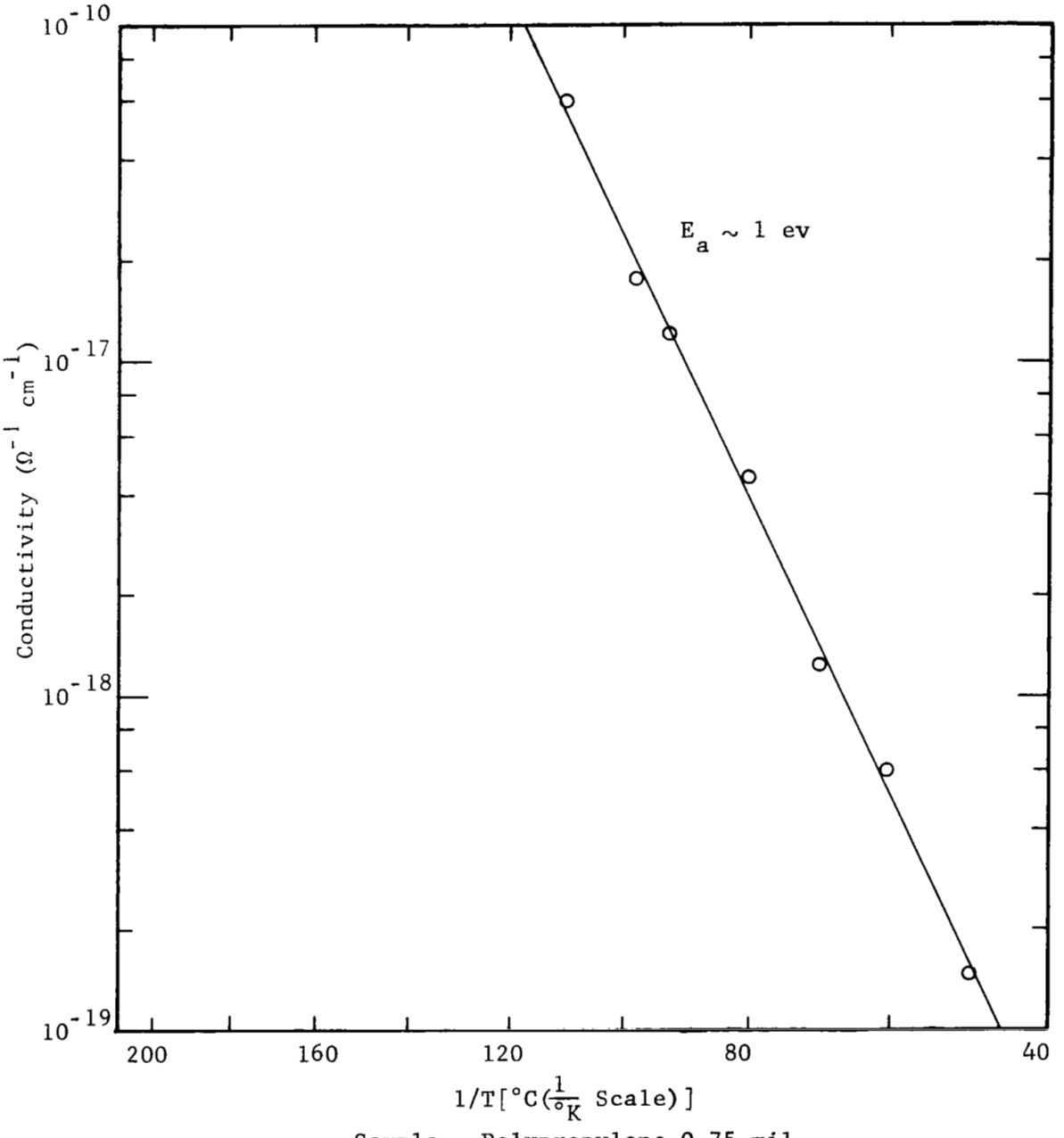

Figure 4.2. Conductivity vs 1/T for 0.75 mil Polypropylene Film

polypropylene and cellulose acetate these current fluctuations occurred at 7.4×10^5 v/cm and 3.9×10^5 v/cm respectively. The self healing nature of these large current fluctuations suggest that a temporary low impedance path occurs in the dielectric which is burned out by the large current flow through the limited area associated with the breakdown. Conceptually, this may occur at defects in the dielectric where the field strength is less than the intrinsic field strength of the material. It is obvious from this discussion that these measurements do not represent the intrinsic field strength, however they do represent a method for correlating the results of the charge storage and thermal release with the observations of spontaneous discharge.

The upturning characteristic which results from the model developed in Chapter II was investigated experimentally in some detail. As indicated, the turn up was observed in most instances after 5×10^3 seconds had elapsed. This effect is shown in Figure 4-3 for two separate samples. The integrating time constant was 10^5 seconds and the characteristics for sample 12G undoubtably are affected by the integrating time constant for $t > 10^4$ seconds. However, all the upturn cannot be explained by the integrating time constant alone. In addition, sample 20G shows an upturning characteristic after 5×10^3 seconds have elapsed. The poor reproducibility from sample to sample of the upturning characteristic is consistent with the poor reproducibility of charge storage from sample to sample. This character of polyethylene terephthalate carries over into the activation energy measurements. Therefore, when the average value shown in Figure 4-1 is used in the model to predict the point where the charge release deviates from the behavior as predicted

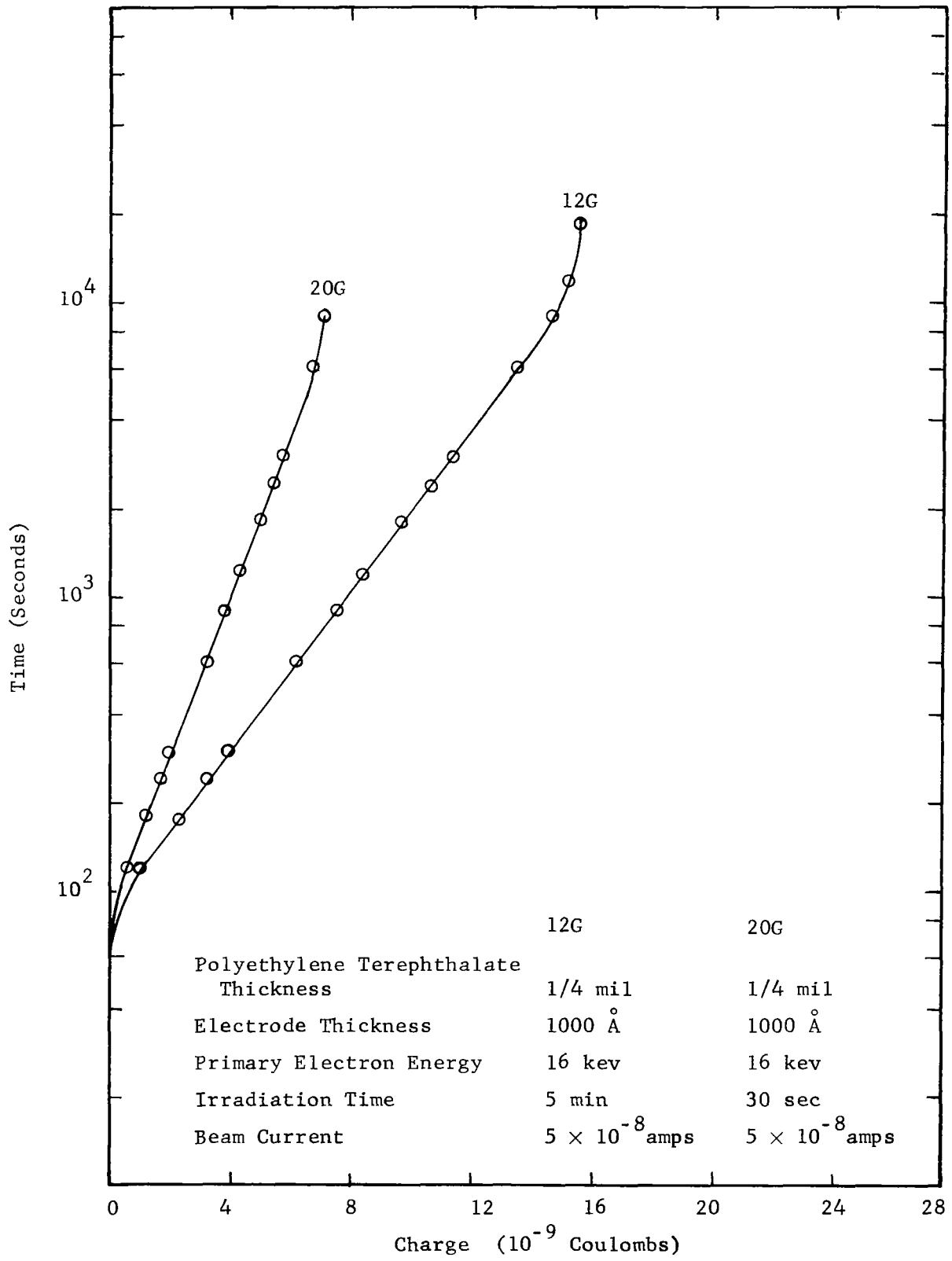

Figure 4.3. Charge Release Measurement Indicating Asymptotic Behavior.

from Equation (B-21), one should expect only an average value. However the average value determined from the model of 1.1×10^3 seconds is somewhat lower than either value shown in Figure 4-3. It may be of interest to further investigate this aspect of charge release with the integrating time constant increased to greater than 10^6 seconds.

One further aspect of charge storage in polyethylene terephthalate was investigated. Charge release measurements were carried out at room temperature and below -100°C with the results shown in Figure 4-4. For the same irradiation time, the same flux rate, and the same electron energy the charge release rate at room temperature is greater than that at -116°C. This result is not surprising since Equation (B-21) predicts that the release of trapped electrons is linearly related to the temperature. Of course this assumes the same number of trapped electrons at $t = 0$. However after warming up the irradiated sample from -116°C to room temperature the total charge released was larger by a factor of 3 over the irradiations carried out at room temperature. Therefore more electrons are trapped at the lower temperatures. It was not practical to pursue these observations in a more detailed manner due to the large temperature variations that occur when one attempts to cool a suspended film. However, the charge storage and thermal release model was qualitatively examined with respect to these observations. As a result the temperature dependence as predicted by Equation (B.21) seems reasonable. In addition the results can be used to obtain a descriptive correlation between the charge release measurements and spontaneous discharge. This is considered in more detail in Chapter V.

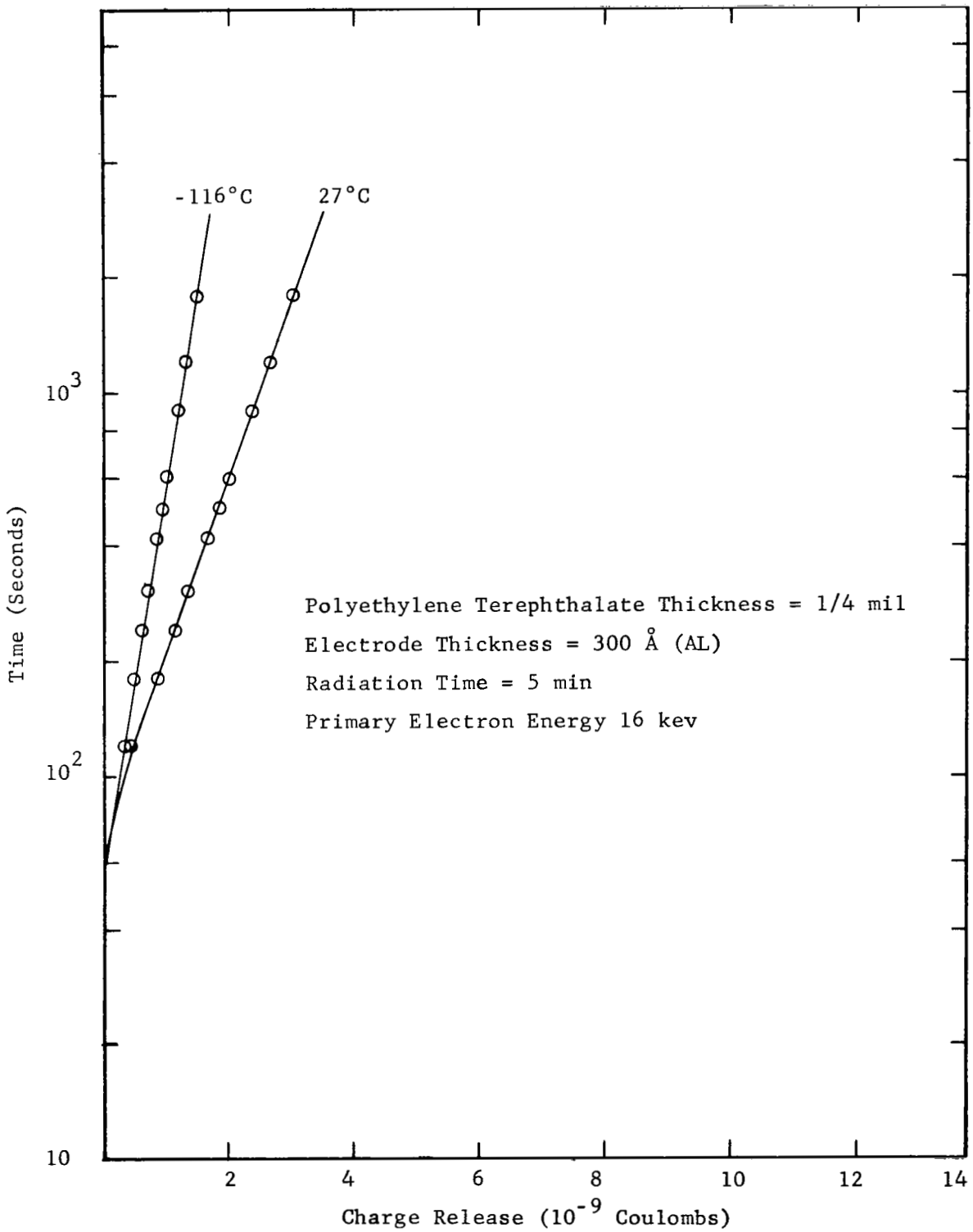

Figure 4.4. Charge Release Measurement at Room Temperature and -116°C.

Charge release measurements on polypropylene and cellulose acetate have also been carried out with the results shown in Figures 4-5 and 4-6. The main purpose was to obtain an estimate of the relative charge storage efficiency of polyethylene terephthalate. If the charge release occurs primarily through simple no-retrapping events, the transfer of external charge is mainly determined by the depth of space charge relative to the thickness of the irradiated sample. For polyethylene terephthalate it was not possible to observe the transfer of external charge for 1.0 mil samples. However for 0.75 mil polypropylene and 1.0 mil cellulose acetate the transfer of external charge was comparable to that for 1/4 mil polyethylene terephthalate. This indicates that the charge storage efficiency for polypropylene and cellulose acetate is much greater than that for polyethylene terephthalate. The marked similarity in the observed charge release characteristics and the charge release model for these films is an additional feature of these results which may be useful for a closer examination of charge storage in polymers.

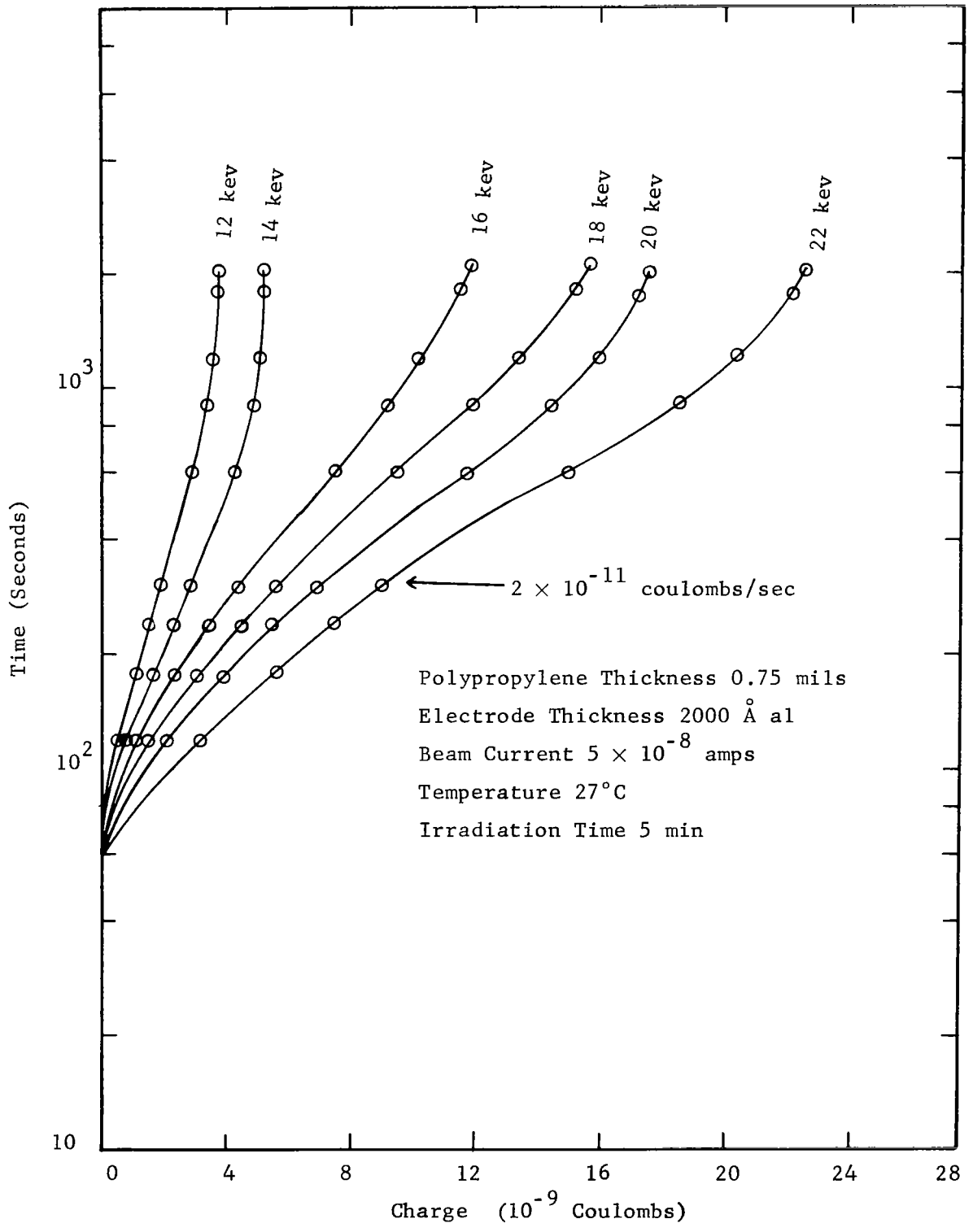

Figure 4-5. Charge Release Measurements for Polypropylene Film.

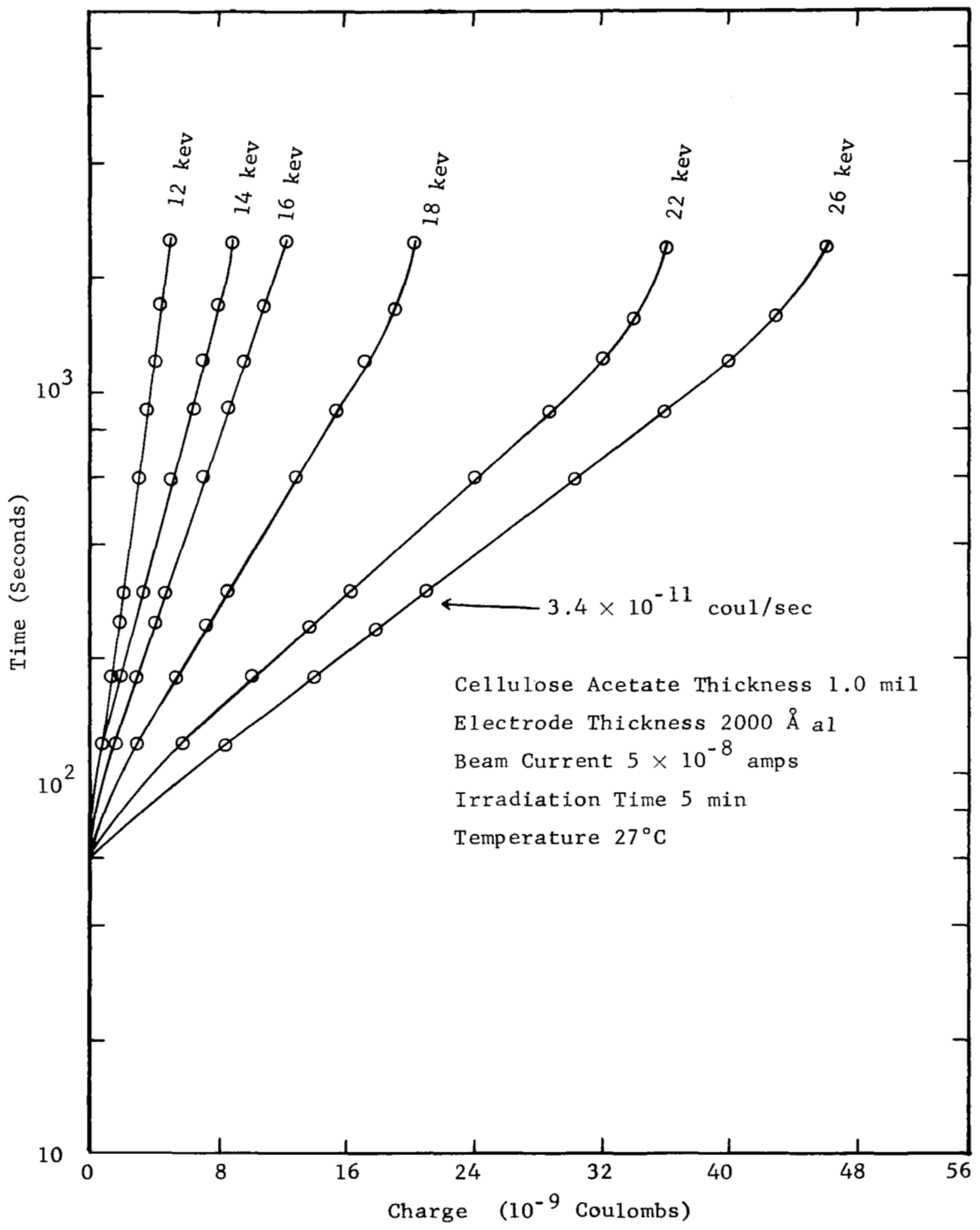

Figure 4.6. Charge Release Measurements for Cellulose Acetate Films.

Chapter V

Discussion and Summary

A phenomenological description of spontaneous discharge associated with electron irradiation of a capacitor-type micrometeoroid detector has been attempted in this report. Measurements of thermally released charge and the observations of spontaneous discharge have been described and it remains to correlate these results. Based upon the simple no-retrapping model for thermal release of irradiation electrons the asymptotic limit indicates a value of internal field of 5×10^5 v/cm. In conjunction with these measurements, an applied field of 5.6×10^5 v/cm was found to overcome the space-charge effect thereby providing a degree of confidence in the charge release model.

A detailed analysis of the spontaneous discharge observations using the ^{147}Pm source has not been possible. This is primarily due to the lack of pulsing. Less than 50% of all samples irradiated yielded pulses. In addition, the results that were obtained indicate that on the average only a small part of the irradiated volume of the sensor is involved in a single discharge event. These results indicate that on the average one requires 3.2×10^{13} e/cm^2-pulse. For 3×10^{14} e/cm^2 using the electron gun the charge release measurements approach the limiting solution. The reproducibility of these measurements was within the sensitivity of the measuring technique. This is an indication that a large volume discharge is not a likely event under the stated irradiation condition. Finally dc field strength measurements where large current fluctuations associated with defect type breakdown were obtained. The value of 6.6×10^5 v/cm is certainly consistent with the charge release measurements

and the concepts which have been associated with the spontaneous discharge observations.

Other aspects of spontaneous discharge associated with electron irradiation of the capacitor-type micrometeoroid detectors have been considered. In general there are insufficient data to provide detailed knowledge. However it seems advisable to present a somewhat subjective analysis of the observations to date for comparison with results obtained by others. Various dc bias levels up to 100 volts were applied to the capacitor structure under irradiation. The bias was applied such that the irradiated electrode was positive for some irradiations and negative for others. There has been no marked charge in the pulsing characteristics. Less than 50% of the samples irradiated under bias pulsed. Also, the pulses were in the millivolt range. Based upon the present data there appears to be no voltage dependence for the pulsing observed for the ^{147}Pm experiment.

Edge effects associated with the geometry of the irradiated sample have been investigated. It was recognized early in the study that bare insulators exposed to the electron flux could obtain a substantial surface charge which could result in a discharge. This has been noted for various insulating materials similar to polyethylene terephthalate. Therefore, the edge of the capacitor structure was always shielded from the primary electron flux. With varying amounts of exposed area (i.e., not metalized) near the edge of the capacitor structure, however shielded from the primary electron flux, no noticeable difference in pulsing characteristics associated with the ^{147}Pm experiment were noted.

For the charge release measurements with samples containing glue between the 1 mil aluminum electrode and the 1/4 mil polyethylene

terephthalate dielectric, preliminary results indicate that the glue stores more charge than polyethylene terephthalate. This statement is predicated on the observation of charge release where the practical range of the primary electrons is beyond the thickness of the irradiated electrode ($\sim 6.25 \times 10^{-5}$ cm) and the polyethylene terephthalate ($\sim 6.25 \times 10^{-4}$ cm). The charge release measurements under these conditions result in an external current which is opposite in sign and much larger than that for polyethylene terephthalate alone. Further interpretation and characterization is complicated due to the composite nature of the irradiated structure. However, it is of interest to the general problem of charge storage in insulating materials and in particular to ambiguous signal generation in the capacitor type micrometeoroid detector to obtain samples where the dielectric region is glue alone.

One area of the present investigation which has not yielded useful data is the attempt to activate the trapped irradiation electrons optically. The primary difficulties are in obtaining an intense source of the proper wavelength (longer than 1 micron) and an electrode material with a low absorption coefficient at the proper wavelength. It has not been possible to pursue the matter in great detail, however it may be necessary to attempt further studies in this area to obtain more information about the distribution of traps with energy.

It has been suggested that proton penetration of the micrometeoroid detector in a space environment may be expected to result in a temporary conducting path established by the high ionization density along the track of the proton. This effect has been considered in a greatly oversimplified manner in Appendix D. The estimates of the parameters

necessary to consider the problem qualitatively are worst case with respect to obtaining a conducting path through the polyethylene terephthalate. The results of the analysis indicate that the effects due to proton irradiation will be quite similar to the electron irradiation effects with respect to ambiguous signal generation.

As a result of these investigations certain aspects of charge storage and spontaneous discharge have been identified where a more detailed knowledge is required. Possibly the most important of these from a practical viewpoint is the reason for less than 50% of the samples pulsing. It is quite possible that the flux rate of the ^{147}Pm is such that an equilibrium between the trapping and thermal release of irradiation electrons occurs which results in an internal field which is insufficient to initiate defect type discharge events. A great deal of understanding in this area can be obtained through the following suggested experimental program.

A. Electron Accelerator Experiment

1. Irradiate structures which show no tendency to pulse when exposed to ^{147} Pm source in order to determine if the structure is also non-pulsing to a high energy monoenergetic flux of electrons.
2. Determine whether environmental testing using a monoenergetic beam is more conducive to pulsing than testing with a distributed energy spectrum source.
3. Correlate pulsing for monoenergetic electron irradiation with electrode thickness and beam current density.

B. Beta Source Experiment

1. Characterize the saturation effect by studying trapping and thermal release of electrons from distributed energy source.

To analyze the data obtained from the charge release measurements one must use a model which implies a phenomenological understanding. Therefore it is necessary to obtain more confidence in the simple no-trapping concept used in the present work. This can be accomplished through the following suggested experimental program associated with the electron gun: (1) obtain a better estimate of the mean range of an electron thermally released from a trap, (2) perform more low temperature measurements to evaluate the temperature dependence of charge release, (3) extend the sensitivity and integration time for the measurement technique, and (4) investigate the trapping and thermal release of irradiation electrons in structures where the thickness of the dielectric can be varied from 0.1 - 5 microns.

Assuming these goals can be obtained one should expect a more detailed insight into the spontaneous discharge event such that ambiguous signal generation associated with electron irradiation of capacitor-type micrometeoroid detectors can be fully evaluated. As a result, one should be able to determine whether or not the capacitor-type structure can be a reliable detector of micrometeoroids in a space environment.

Appendix A

Transfer to External Charge Due to Space Charge Decay

For a distribution of trapped electrons which varies with distance through the media and is uniform in cross section, a one dimensional solution of Poisson's equation for a slowly varying charge distribution

$$\frac{\partial E(x,t)}{\partial x} = - \frac{q}{\epsilon} \bar{n}_t(x,t) \qquad (A.1)$$

describes the electrical field within the material where $\bar{n}_t(x,t)$ is the net charge distribution in the polyethylene terephthalate film. Referenced to the zero field point x_o which is a function of time and positive x as shown in Figure 2.8, one can describe the electric field distribution by

$$E(x,t) = - \frac{q}{\epsilon} \int_{x_o(t)}^{x} \bar{n}_t(x,t)\, dx \ . \qquad (A.\ )$$

for a sample of thickness d and the electrodes grounded

$$\int_o^d E(x,t)dx = - \int_o^d \int_{x_o(t)}^{x} \frac{q}{\epsilon} \bar{n}_t(\tilde{x},t)\, d\tilde{x}dx = 0 \qquad (A.3)$$

or

$$\int_o^d \int_{x_o(t)}^{x} \bar{n}_t(\tilde{x},t)\, d\tilde{x}dx = 0 \ .$$

This can be used to determine the zero field point for a given distribution $\bar{n}_t(x,t)$. The surface charge density at the unirradiated electrode can be expressed as

$$\sigma(x',t) = D(x',t) = -\epsilon E(x',t) = q \int_{x_o(t)}^{x'} \bar{n}_t(x,t)dx \qquad (A.4)$$

where the upper limit corresponds to the electrode of interest. As the

space charge decays, the surface charge changes according to Equation (A.4). If the space charge on both sides of the zero-field point decays proportionally in time, there will be no external transfer of charge between the electrodes. However, if the decay results in net charge pairs on the electrodes, external charge transfer will occur and can be expressed in terms of the moving zero-field point. The total change in surface charge with respect to time is

$$\frac{dQ(x',t)}{dt} = qA\left[\int_{x_o(t)}^{x'} \frac{\partial \bar{n}_t(x,t)}{\partial t}\, dx - \bar{n}_t(x_o,t)\,\frac{dx_o}{dt}\right] . \qquad (A.5)$$

The surface charge at the electrode boundaries can be expressed by

$$Q(x',t) = -\,qA\left[\int_{x_o(o)}^{x_o(t)} \bar{n}_t(x_o,t)\,dx_o - \int_o^t \int_{x_o(t)}^{x'} \frac{\partial \bar{n}_t(x,t)}{\partial t}\, dx\,dt\right] + Q(x',0) \qquad (A.6)$$

where the first term represents the net charge pairs which must be transferred through the external circuit, the second term represents the space charge which reaches the unirradiated electrode and the third term represents the surface charge on the unirradiated electrode at $t = 0$. Therefore, the transfer of external charge can be expressed as

$$dQ_{ext}(t) = qA\bar{n}_t(x_o,t)\,dx_o . \qquad (A.7)$$

The difficulty in applying Equation (A.7) usually involves the distribution $\bar{n}_t(x_o,t)$.

In some instances an approximation to the maximum value for Equation (A.7) can be obtained by assuming that all the electrons released from traps arrive at the irradiated electrode without being retrapped. For the present work the trapped electron distribution resulting from the

stopping of primary electrons and the injection of secondaries from the electrodes will be assumed to be uniform with distance into the polyethylene terephthalate film extending from the irradiated surface to the practical range of the primaries. The geometry of the irradiated sample is shown in Figure 3-1. For the stated assumptions the maximum external charge transfer will depend upon the surface charge density (σ_2) on the unirradiated electrode. Furthermore, assuming irradiation has ceased and that net charge pairs can flow through an external circuit

$$Q_{ext}(max) = A_1\sigma_2 = A_1\epsilon \left|E\right|_{x=d} \qquad (A.8)$$

where $\left|E\right|_{x=d}$ is the magnitude of the electric field at the polyethylene terephthalate boundary at the unirradiated electrode.

To calculate the electric field resulting from trapped irradiation electrons, consider the simple model in Figure 3-1 where the diameter of the irradiated area A_1 is much greater than the thickness d. Electrons are injected at x = 0, uniformly across the area A_1. It is assumed that all of these electrons are stopped within a distance d_1 in the polyehtylene terephthalate and result in a uniform charge density ρ for $x < d_1$ and charge density zero for $x > d_1$. There by Poisson's equation

$$\nabla^2 V = -\frac{\rho}{\epsilon} \qquad 0 \leq x < d_1 \qquad (A.9)$$

$$\nabla^2 V = 0 \qquad d_1 < x \leq d \ . \qquad (A.10)$$

Using the boundary conditions that the potential is zero at the extreme boundaries

$$V(0) = V(d) = 0$$

and that the displacement vector is continuous across the boundary at $x = d_1$, the electric field in these two regions is

$$E = - \frac{q\bar{n}_t}{\epsilon} \left[x = \frac{d_1}{d} \left(d - \frac{d_1}{2}\right)\right] \qquad 0 \leq x \leq d_1 \tag{A.11}$$

$$E = - \frac{qn_t d_1^2}{2\epsilon d} \qquad d_1 \leq x \leq d \ . \tag{A.12}$$

Therefore

$$Q_{ext}(max) = \frac{qA_1\bar{n}_t d_1^2}{2d} \ . \tag{A.13}$$

Equation (A.13) can be used to reflect the asymmetry considerations for the stated assumptions when one is interested in the release of electrons from traps over a time interval which permits most of the space charge to decay toward a charge neutral condition throughout the polyethylene terephthalate film.

Appendix B

Thermal Release of Trapped Electrons

For a single trapping level the decay of trapped electrons where retrapping is negligible may be written as

$$\frac{dn_t(x,t)}{dt} = - n_t(x,t)\ P \qquad (B.1)$$

where P is the probability of an electron escaping from a trap site. The simple solution for P independent of time is

$$n_t(x,t) = n_t(x,0)e^{-Pt} \ . \qquad (B.2)$$

If the energy level of a trapped electron is E ev below the conduction band the electron must absorb at least E ev of thermal energy before it can escape the trap. The probability P of an electron escaping from a trap of depth E at temperature T is of the form

$$P = s\ e^{-E/kT} \qquad (B.3)$$

where s is an attempt to escape frequency determined by the number of times per second that the electron can absorb energy and $e^{-E/kT}$ is the Boltzmann factor representing the probability that an electron will have the necessary energy to be freed from the trap. For polyethylene terephthalate a value of $s = 9 \times 10^{10}$ seconds^{-1} has been determined from x-ray induced conductivity studies.[14] Therefore the number of electrons per cm^3 in traps may be expressed as

$$n_t(x,t) = n_t(x,0)\ e^{-ste^{-E_t/kT}} \qquad (B.4)$$

where E_t is the trap depth measured from the conduction band.

If the trapping sites are distributed in energy such that a continuous function can be used to denote the number per cm^3 per electron volt below the conduction band, an expression analogous to Equation (B.4) can be obtained. For each unit energy level below the conduction band the number of trapped electrons per cm^3 is

$$\frac{dn_t(x,t)}{dE} = \frac{dn_t(x,0)}{dE} e^{-ste^{-E/kT}} . \tag{B.5}$$

The number of trapped electrons per cm^3 at t = 0 as a function of position in the material can be obtained in terms of quasi-Fermi level $E_{fn}(x)$ assuming the trap distribution N_t is known. The quasi-Fermi level corresponds to the energy with respect to conduction band of the highest filled trapping levels and is a function of position. Using these concepts

$$n_t(x,0) = \int_{E_{fn}(x)}^{E_{fo}} \frac{dN_t}{dE} dE \tag{B.6}$$

where E_{fo} is the equilibrium Fermi level for dark conductivity. Combining Equations (B.5) and (B.6) and integrating with respect to energy yields

$$n_t(x,t) = \int_{E_{fn}(x)}^{E_{fo}} \frac{dN_t}{dE} e^{-ste^{-E/kT}} dE . \tag{B.7}$$

Qualitative descriptions of photoconductive processes,[28] space charge decay[29] and x-ray induced conductivity[14] have been obtained for various materials using a uniform distribution where

$$\frac{dN_t}{dE} = \frac{B}{kT_c} . \tag{B.8}$$

The constant B/kT_c appears in this particular form as a matter of convience in the present work.

For the uniform distribution one obtains using Equations (B.7) and (B.8)

$$n_t(x,t) = \int_{E_{fn}(x)}^{E_{fo}} \frac{B}{kT_c} e^{-ste^{-E/kT}} dE \quad . \tag{B.9}$$

Using the assumption of uniform trapping from the irradiated surface to the practical range r_o of the primary electrons, the quasi-Fermi level is constant for $x < r_o$ and $E_{fn}(x) = E_{fo}$ for $x > r_o$. Using this result, and introducing a change in variable where $y = ste^{-E/kT}$ for $x < r_o$,

$$n_t(t) = \frac{BT}{T_c} \int_{ste}^{ste^{-E_{fn}/kT}} \frac{e^{-y}}{y} dy \quad . \tag{B.10}$$

Denoting $st = a$, $e^{-E_{fn}/kT} = \beta$, $e^{-E_{fo}/kT} = \alpha$, and $T/T_c = m$, one obtains

$$n_t(t) = Bm \int_{a\alpha}^{a\beta} \frac{e^{-y}}{y} dy \quad . \tag{B.11}$$

This can also be expressed as

$$\frac{n_t(t)}{Bm} = \int_{a\alpha}^{\infty} \frac{e^{-y}}{y} dy - \int_{a\beta}^{\infty} \frac{e^{-y}}{y} dy \tag{B.12}$$

which results in the difference between two exponential integrals where numerous tabulated solutions exist.[30] Before indicating the solutions of interest, the limiting values should be investigated. Referring to Equation (B.9) one readily sees that

$$\lim_{t\to 0} n_t(x,t) = \frac{B}{kT_c}\left[E_{fo} - E_{fn}(x)\right] \quad , \tag{B.13}$$

and $\lim_{t\to\infty} n_t(x,t) = 0$.

A generalized solution for Equation (B.12) can be conveniently obtained by relating the lower limits of integration. For all values of $t \to 0$, the limits are related by a constant depending upon the energy difference between the equilibrium Fermi level and the quasi-Fermi level. Denoting the ratio $\frac{\beta}{\alpha} = \gamma$ Equation (B.12) can be written as

$$\frac{n_t(t)}{Bm} = \int_{a\alpha}^{\infty} \frac{e^{-y}}{y}\, dy = \int_{a\gamma\alpha}^{\infty} \frac{e^{-y}}{y}\, dy \qquad t > 0 \ . \tag{B.14}$$

A family of solutions can be obtained after one determines the range of interest for the lower limit of integration $a\alpha$ in the first integral. A plot of the solution to the first integral is shown in Figure B-1 where $\gamma \geq 10^4$ and $10^{-3} \leq a\alpha \leq 1$. For $t > 60$ seconds and $s = 9 \times 10^{10}$ $second^{-1}$, this solution applies for equilibrium Fermi-level values in the range from 0.75 ev to 0.95 ev. Solutions for Equation (B.14) for values of $\gamma < 10^4$ are of interest and can be obtained by taking the difference between the portions of the curve for $\gamma \geq 4$ which correspond to the solutions of the two integrals. This procedure was used to generate the family of curves where γ is a parameter.

Using Figure B-1, the thermally released electrons per cm^3 can be determined as a function of time. In general it is inconvenient to observe the space charge decay immediately after electron irradiation has ceased. The elapsed time (τ) is determined by practical considerations. Therefore the electrons per cm^3 thermally released as a function of time during the measurement period is

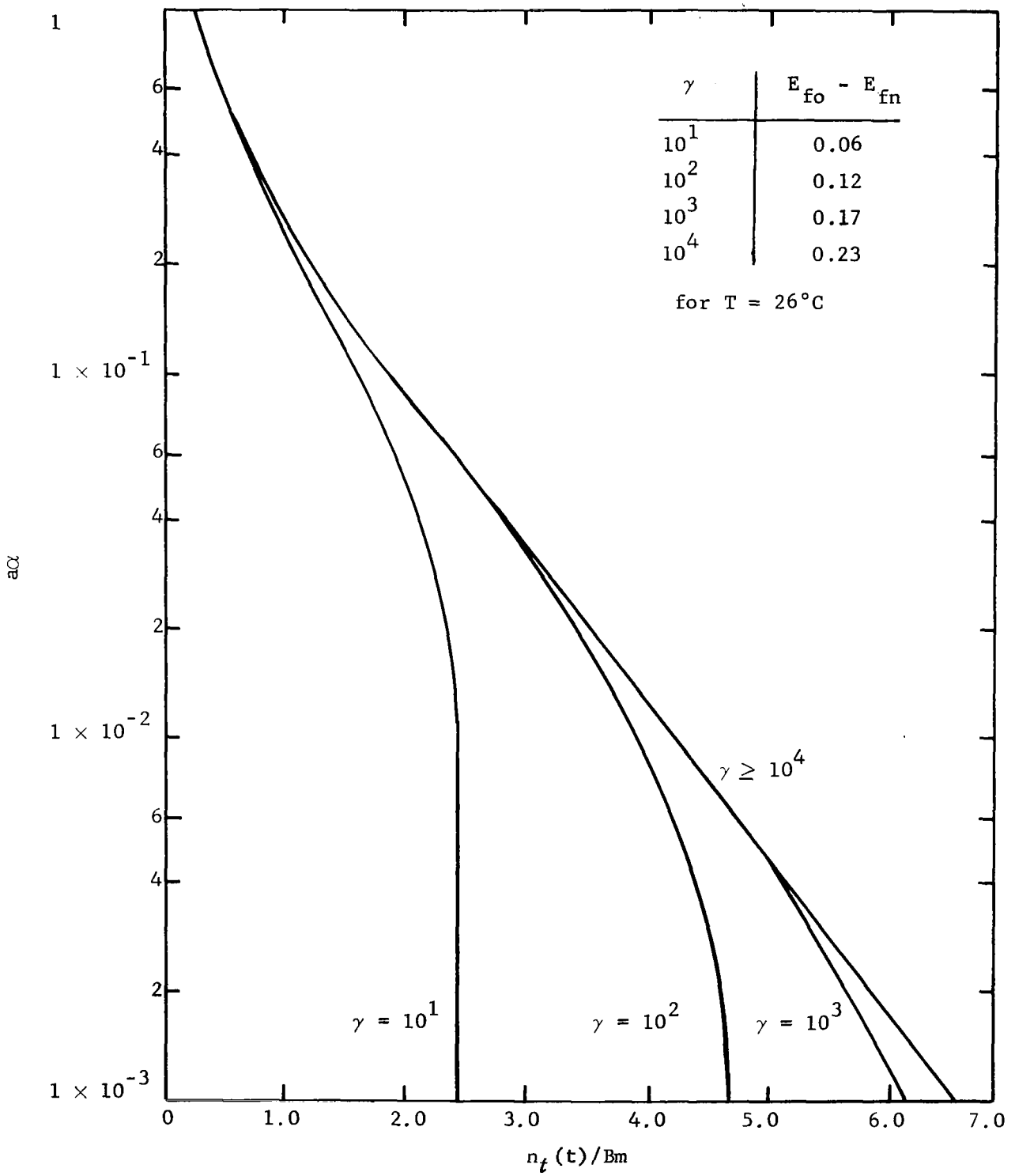

Figure B-1. Normalized Trapped Electron Density vs Normalized Time for Uniformly Distributed Trap Density.

$$n_r(t) = n_t(\tau) - n_t(t) \qquad t \geq \tau \tag{B.15}$$

as shown for normalized values in Figure B-1. Although the variables are normalized, the results clearly indicate the dependency of the released charge upon γ.

It is possible to obtain an approximate solution for $n_r(t)$ if $\gamma \geq 10^4$ and $0.001 \leq a\alpha \leq 0.1$. Under these conditions the second integral in Equation (B.12) can be neglected with respect to the first integral. Therefore

$$\frac{n_t(t)}{Bm} \simeq \int_{a\alpha}^{\infty} \frac{e^{-y}}{y}\, dy \qquad 0.001 \leq a\alpha \leq 0.1 \ . \tag{B.16}$$

Carrying out the integral in two parts to obtain

$$\frac{n_t(t)}{Bm} \simeq \int_{a\alpha}^{0.1} \frac{e^{-y}}{y}\, dy + \int_{0.1}^{\infty} \frac{e^{-y}}{y}\, dy \qquad 0.001 \leq a\alpha \leq 0.1 \tag{B.17}$$

and introducing the value of the definite integral from tables[29] yields

$$\frac{n_t(t)}{Bm} \simeq \int_{a\alpha}^{0.1} \frac{e^{-y}}{y}\, dy + 1.8 \qquad 0.001 \leq a\alpha \leq 0.1 \ . \tag{B.18}$$

The remaining integral can be integrated by parts to yield the series

$$\int \frac{e^{-y}}{y}\, dy = \ell n\ y + \frac{y}{1!} + \frac{y^2}{2!} + \ldots . \tag{B.19}$$

For $0.001 \leq a\alpha \leq 0.1$ only the first term of the series is needed for the accuracy desired. Therefore

$$\frac{n_t(t)}{Bm} \simeq -0.5 - \ell n\ a\alpha \ . \tag{B.20}$$

Following the procedure of Equation (B.15), and recalling the definition

a = st the electrons released per cm^3 as a function of time for $\gamma \geq 10^4$ can be expressed as

$$n_r(t) = Bm \ \ell n \frac{t}{\tau} \quad , \quad \left[\begin{array}{c} \frac{0.001}{s\alpha} \leq t \leq \frac{0.1}{s\alpha} \\ \\ \frac{0.001}{s\alpha} \leq \tau \leq \frac{0.1}{s\alpha} \end{array} \right] \quad , \quad t \geq \tau \ . \qquad \text{(B.21)}$$

This solution corresponds to the curve for $\gamma \geq 10^4$ in Figure B-2, and will prove useful in inferring certain aspects of electron trapping for the uniform distribution of traps.

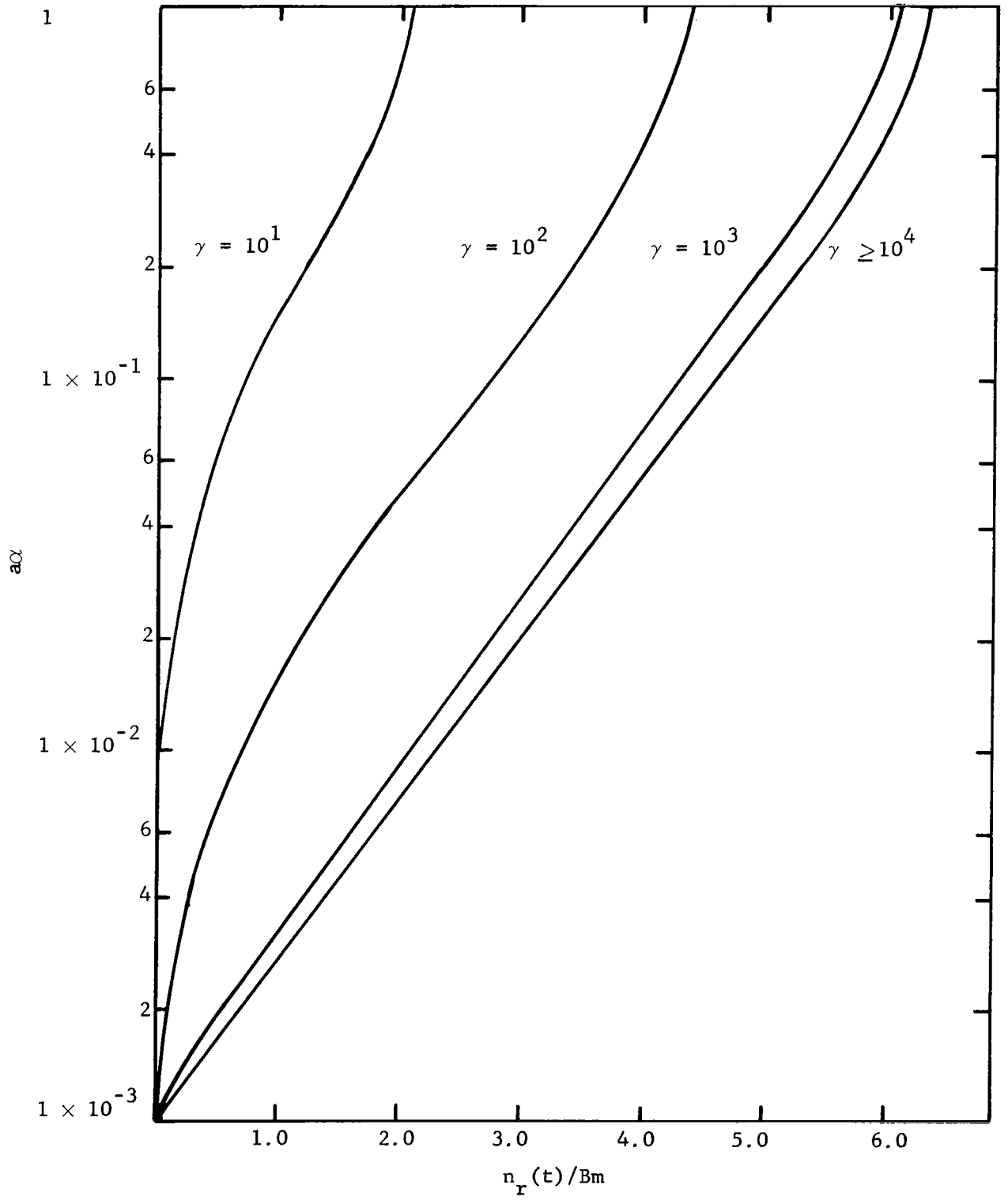

Figure B-2. Normalized Thermal Release of Trapped Electron Density vs Normalized Time for Uniformly Distributed Trap Density.

Appendix C

β-Flux Calculations for the ^{147}Pm Source

C.1 Energy Spectrum

The differential energy spectrum for the ^{147}Pm source of Figure 3.6 was supplied by Oak Ridge National Laboratory. The total activity originally supplied was nominally 70 curies ($S_o = 2.6 \times 10^{12}$ e/sec). Ideally the shape of the low energy spectrum could be approximated by extrapolating the slope at around 25 kev. In practice, however, one obtains a considerable number of secondary electrons of negligible penetrating power which are ejected from the surface of the source. Current measurements such as those from a Faraday cage in a vacuum would measure these electrons whereas a particle detector would not observe them due to the thickness of its dead layer. Thus the differential energy spectrum is critical in comparing the response of one detection method to another.

C.2 Faraday Cage Current Measurements

Since β-particles eventually slow down to thermal electrons, the total flux can be determined by current measurements in a good geometry system. Such a system is the Faraday cage shown in Figure C-1. The current passing through the small hole of diameter D is given by the equation

$$I = S_o G f_b e^{-u_o x_o} e^{-.693\ t/T_{1/2}} \qquad (C.1)$$

where S_o - total activity of the source at the date of fabrication,

t - time after fabrication,

$T_{1/2}$ - decay half-life of source,

$e^{-u_o x_o}$ - self absorption and attenuation of source covering,

f_b - backscatter factor (for ^{147}Pm on magnesium silicate or aluminum $f_b \sim 1.17$),

G - geometry efficiency.

The geometry efficiency for a point source is given by

$$g = \frac{g\Omega}{4\pi}$$

where $d\Omega$ is the solid angle intercepted by the detector. Thus for a surface distributed source the geometry efficiency is given by

$$G = \frac{\int_A gs\,dA}{\int_A s\,dA} \tag{C.2}$$

$$G = \frac{\int_A gs\,dA}{S_o} \tag{C.3}$$

where s = surface density of the source.

For uniform distribution it is simply

$$G = \frac{\int_A g\,dA}{A} \quad . \tag{C.4}$$

For the geometry of Figure C.1 where

$$D \ll d$$

and

$$\rho_o \ll d$$

we obtain

$$G = \frac{D^2}{16d^2}\left[\frac{1 - \frac{1}{4}\frac{\rho_o^2}{d^2}}{1 + \frac{1}{2}\frac{\rho_o^2}{d^2}}\right] \quad . \tag{C.5}$$

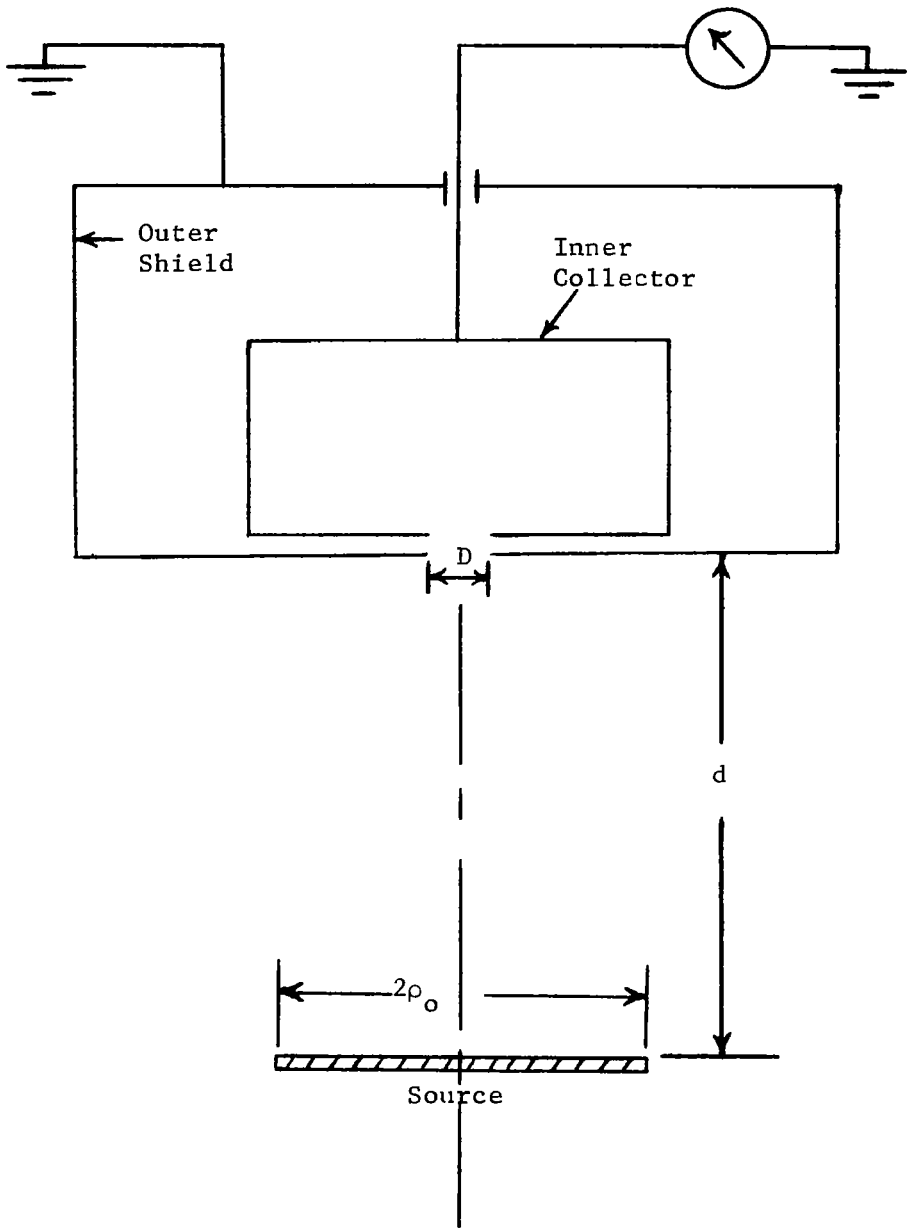

Figure C-1. Cross Section of Faraday Cage Arrangement for Measurement of β-flux.

Calculate G:

$$D = 1/8"$$

$$\rho_o = 1"$$

$$d = 5\ 3/4"$$

$$G = \frac{1}{16(33.06)64}\left[\frac{1 - \frac{1}{4(33.06)}}{1 + \frac{1}{2(33.06)}}\right]$$

$$= .289 \times 10^{-4}$$

The undetermined factor is $S_o e^{-u_o x_o}$, but we can assume the nominal value for S_o. From Equation (C.1)

$$e^{-u_o x_o} = \frac{Ie^{.693\frac{t}{T_{1/2}}}}{S_o G f_b} \quad . \tag{C.6}$$

We can now calculate the self absorption term if we measure the current passing through the hole in the Faraday cage. Using the following values

$$I = .24 \times 10^{-11} \text{ amp}$$

$$e^{-.693t/T_{1/2}} = 0.81$$

$$S_o = 2.6 \times 10^{12} \text{ e/sec}$$

$$G = .289 \times 10^{-4}$$

$$f_b = 1.17$$

we obtain

$$e^{-u_o x_o} = 0.210 \ .$$

Let us define ξ:

$$\xi = S_o e^{-u_o x_o} f_b e^{-0.693\frac{t}{T_{1/2}}} \quad . \tag{C.7}$$

Then ξ is the effective source activity. From the above results we get

$$\xi = 13.8 \text{ curies} .$$

C.3 Calculations for Circular Disk Source and Sample

The parameters of Figure C-2 are used to compute the geometry efficiency for a source and sample having the shape of a circular disk.

When $\gamma < 1$ and $c < b$ we can use the following equation which is the first terms of a power series of γ.[31]

$$G = 0.5\left[1 - \frac{1}{(1+\beta)^{1/2}} - \frac{3\beta\gamma}{8(1+\beta)^{5/2}} - \gamma^2\left(-\frac{5\beta}{16(1+\beta)^{7/2}} + \frac{35\beta^2}{64(1+\beta)^{9/2}}\right)\right.$$

$$\left. - \gamma^3\left(\frac{35\beta}{128(1+\beta)^{9/2}} - \frac{315\beta^2}{256(1+\beta)^{11/2}} + \frac{1155\beta^3}{1024(1+\beta)^{13/2}}\right)\right] . \qquad (C.8)$$

For the particular case where $c > b$ we use the exact expression for G.[32]

$$G = \frac{1}{2}\left[\frac{\beta}{\gamma}\left(1 - \frac{1}{\sqrt{1+(\gamma-\beta)^2}}\right) + \frac{1}{2}\left(\frac{1}{\sqrt{1+(\gamma-\beta)^2}} - \frac{1}{\sqrt{1+(\gamma+\beta)^2}}\right)\right]$$

$$+ \frac{1}{\pi c\gamma}\int_{c-b}^{b+c}\left\{\frac{b^2}{2}\cos^{-1}\left(\frac{R^2+b^2-c^2}{2Rb}\right) - \frac{c^2}{2}\sin^{-1}\left(\frac{R^2+c^2-b^2}{2Rc}\right)\right.$$

$$\left. - \frac{1}{4}\sqrt{4R^2b^2 - (R^2+b^2-c^2)^2}\right\}\frac{RdR}{(R^2+a^2)^{3/2}} . \qquad (C.9)$$

The integral is evaluated numerically.

Current measurements were taken from a plate having the geometry of Figure C.2 and compared with predictions based on the Faraday cage measurements. The critical dimensions were

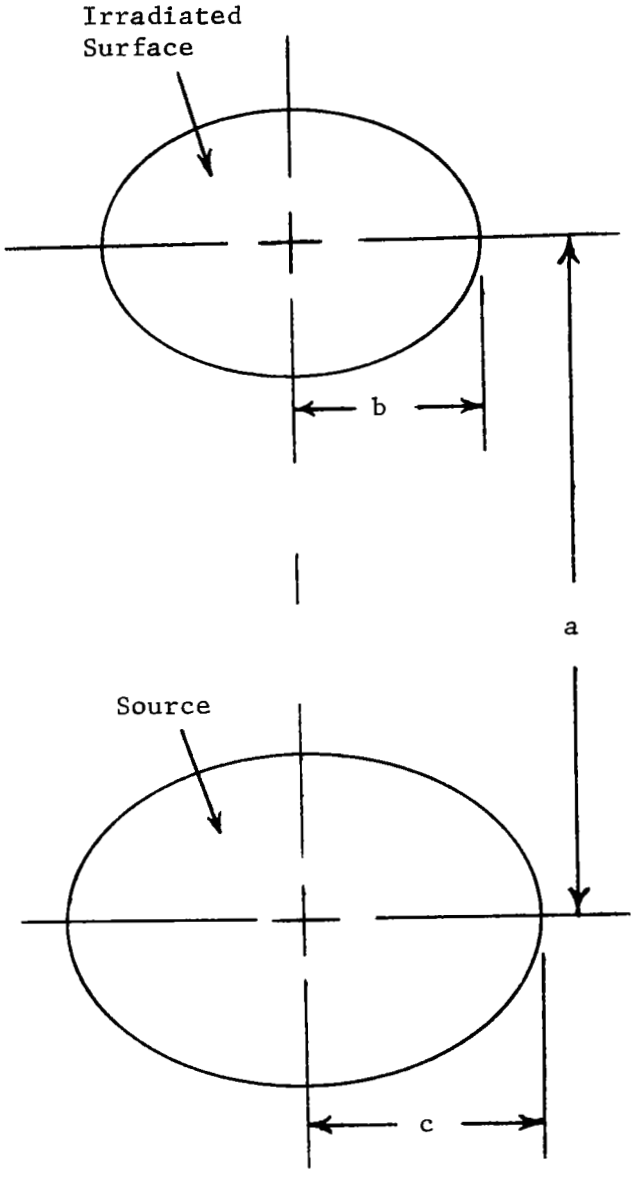

Figure C-2. Geometry for Disk Source and Irradiated Surface.

$$a = 11\ 7/8"$$

$$b = 3"$$

$$c = 1"$$

resulting in a value of G = 0.0154.

$$I_{calc.} = G\xi \ . \qquad (C.10)$$

ξ is found by Equation (C.7) to be 13.8 curies or 0.511×10^{12} e/sec.

$$I_{calc} = 0.0154 \times 0.511 \times 10^{12} \times 1.6 \times 10^{-19} \text{ amp}$$

$$I_{calc} = 1.26 \times 10^{-9} \text{ amp} \ .$$

The measured current was

$$I_{meas} = 1.2 \times 10^{-9} \text{ amp} \ .$$

Therefore current measurements on a bare disk compare favorably with the current measurements of the Faraday cage and can be used to indicate the electron flux in the sample. This is convenient when the source and detector are very close because of the difficulty of solving Equations (C.8) and (C.9).

Appendix D

Ambiguous Signal Generation Due to Proton Irradiation

With respect to the discharge along the tract of a proton, one can at least propose an analog which will allow qualitative arguments. Assuming the charge that is stored on the electrodes of the capacitor is to be transported through the ionization track of a proton, the conductivity of the path will determine the magnitude of the discharge pulse since the time constant of discharge is the product of the capacitor of the detector and the resistance of the discharge path. Of course the limiting value for the discharge pulse amplitude is determined by the ratio of the time constant of the discharge path and the lifetime of the ionized media. For this simple interpretation the time constant for discharge can be written as

$$T = \frac{\epsilon A}{n q \mu a}$$

where $\epsilon \approx 2.6 \times 10^{-13}$ farads/cm

A = electrode area in cm^2 ($\approx 100\ cm^2$)

n = carrier density along the track of the proton ($\approx 10^{20}$ along the tract of a fission fragment in silicon)

q = electronic charge

$\mu \approx$ mobility of carrier (Fowler's estimate by x-ray induced conductivity studies $10^{-3}\ cm^2\ V^{-1}\ sec^{-1}$)

a = cross section of the columnar ionization

Using the aforementioned values which represent a conservative estimate of T one finds

$$T \approx \frac{10^{-7}}{a} .$$

The total lifetime of free electrons (τ) in contributing to the conduction lies between 10^{-7} and 10^{-9} seconds for polyethylene terephthalate as estimated by Fowler.[2] Therefore the ratio $\tau/T \approx a$. The interpretation of this analog depends upon the extension of the ionization along the track of the proton. In addition, it is assumed that this extension can be characterized by an effective distance within which the density of ionized carriers is approximately 10^{20} cm^{-3}. A reasonable upper limit for "a" based on the aforementioned restraints is 10^{-4} cm^2. Using these approximations one finds

$$\frac{\triangle Q}{Q_o} = (1 - e^{-\tau/T}) \sim 1 - \frac{\tau}{T}$$

or a charge transport ($\triangle Q$) less than 0.01% of the stored charge (Q_o). Therefore, it appears that an individual proton track will not yield a significant discharge pulse.

The next consideration is for a flux of protons with sufficient energy to penetrate the detector. Assuming the flux to be 10^4 protons/cm^2 sec there would be a charge drain of less than 1%/sec since it is anticipated that the recharge time constant is considerably less than 1 sec and more like 10^{-4} seconds. Again the charge deviation on the electrodes will draw a small amount of charge from the power supply.

It is quite obvious that this discussion is greatly oversimplified. First the ionization track acts more like a plasma in a strong electric field so that conduction through the plasma does not occur precisely as has been described. Secondly, there will be recombination along the

plasma which will reduce the charge density. Thirdly the columnar ionization will not be uniform over the assumed dimensions but will decrease from the value along the track out to the path length of the δ-rays. Lastly, collection of the more mobile carrier at one of the electrodes and trapping of both the hole and electron will reduce transport through the detector of the charge stored on the electrodes. All of the factors will tend to reduce the magnitude of a discharge pulse assumed to originate through the mechanism of a temporary conducting path established by the high ionization density along the tract of the proton.

One should consider the charge that can be collected by the electric field in the detector analogous to semiconductor nuclear particle detectors. However the carrier lifetime is so short ($< 10^{-7}$ sec) and trap density so high ($> 10^{16}$ cm^{-3}) that its response to charge particles would be quite complicated. However, one would not intuitively expect the charge collection efficiency to approach that for semiconductor nuclear particle detectors. The voltage pulse appearing across the detection electronics for the charge sensing technique is

$$V = Q/C_{tot}$$

where Q is the total charge liberated by the particle in the depletion region and C_{tot} is the sum of the detector capacitance and external shunt capacitance. For protons in the range of interest the voltage pulse into about 50 pf would be in the millivolt range. Therefore

$$Q_c \sim 50 \times 10^{-12} \times 10^{-3} = 5 \times 10^{-14} \text{ coulombs}$$

are collected. The charge stored on a 10^{-8} farad detector biased at 10 volts is

$$Q_B = 10^{-7} \text{ coulombs}$$

so that the deviation is again insignificant with respect to the sensitivity desired to detect the pulses from micrometeoroid impact.

Problems which seem more significant with respect to proton irradiation are the secondary electrons injected from the aluminum front plate and ionized charge trapping in the mylar. However each of these effects is considered in the electron irradiation study and it appears from present data that the protons will have about the same effect in terms of spurious counts. The shape of the pulse, its occurrence and amplitude will be similar to the electron initiated pulse for these charge storage mechanisms.

REFERENCES

1. L. K. Monteith (to be published).

2. J. F. Fowler, "X-Ray Induced Conductivity in Insulating Materials", Proc. Royal Soc. A236, 1956, p. 464.

3. J. V. Pascale, D. B. Herrmann and R. J. Miner, "High-Energy Electron Radiation Resistance of Plastics", Modern Plastics, October 1963.

4. Mrs. S. D. Burow, D. T. Turner, G. F. Pezdirtz and G. D. Sands, "Degradation of Polyethylene Terephthalate by X-Radiation", Polymer Preprints, 1964, p. 396.

5. K. Yahagi, "Gamma-Ray Induced Conductivity in Polyethylene and Teflon Under Radiation at High Dose Rate", J. Appl. Phys. 34, April 1963, p. 804.

6. K. G. McKay, "Electron Bombardment Conductivity in Diamond. Part I", Phys. Rev. 74, 1948, p. 1606.

7. K. G. McKay, "Electron Bombardment Conductivity in Diamond. Part II" Phys. Rev. 77, March 1950, p. 816.

8. A. J. Ahearn, "Conductivity Induced in Diamonds by Alpha Particle Bombardment and Its Variations Among Specimens", Phys. Rev. 73, 1948, p. 1113.

9. L. Pensak, "Conductivity Induced by Electron Bombardment in Thin Insulating Films", Phys. Rev. 75, February 1949, p. 472.

10. P. V. Murphy and S. C. Ribeiro, "Polarization of Dielectrics by Nuclear Radiation. I. Release of Space Charge in Electron Irradiated Dielectrics", J. Appl. Phys. 34, July 1963, p. 2061.

11. B. Gross, "Irradiation Effects in Borosilicate Glass", Phys. Rev. 107, July 1957, p. 368.

12. B. Gross, "Irradiation Effects in Plexiglas", J. Polymer Sci. 27, 1958, p. 135.

13. B. Gross and P. V. Murphy, "Electrical Irradiation Effects in Solid Dielectrics", Nukleonik 2, 1961, p. 279.

14. J. H. Fowler, "X-Ray Induced Conductivity in Insulating Materials", Proc. Roy. Soc. (London) A236, 1956, p. 464.

15. F. Gutmann, "The Electret", Rev. of Mod. Phys. 20, July 1948, p. 457.

REFERENCES (continued)

16. J. R. Freemon, H. P. Kallmann and M. Silver, "Persistent Internal Polarization", Rev. of Mod. Phys. 33, October 1961, p. 553.

17. P. V. Murphy, S. C. Ribeiro, F. Milanez and R. J. de Moraes, "Effect of Penetrating Radiation on the Production of Persistent Internal Polarization in Electret-Forming Materials", J. Chem. Phys. 38, May 1963, p. 2400.

18. E. J. Stunglass, "Backscattering of Kilovolt Electrons from Solids", Phys. Rev. 95, July 1954, p. 345.

19. H. Kanter, "Energy Dissipation and Secondary Electron Emission in Solids", Phys. Rev. 121, February 1961, p. 677.

20. Mylar, a trade name of DuPont.

21. W. H. Barkas and M. J. Berger, Tables of Energy Losses and Ranges of Electrons and Positrons, Office of Technical Services, Department of Commerce, Washington, D. C., 1964, NASA SP-3012.

22. J. R. Young, "Dissipation of Energy by 2.5 - 10 kev Electrons in Al_2O_3", J. Appl. Phys. 28, May 1957, p. 524.

23. L. V. Spencer, Energy Dissipation by Fast Electrons, NBS Monograph 1, Washington, D. C., U. S. Government Printing Office, 1959.

24. S. M. Kirov Tomsic Polytechnic Institute, "On the Mechanism of the Electric Breakdown of Solid Dielectrics", by G. A. Vorob'yev, USSR, October 1960, N63-13621.

25. Y. Inuishi and O. A. Powers, "Electric Breakdown and Conduction Through Mylar Films", J. Appl. Phys. 28, September 1957, pp. 1017-1022.

26. Emanuel L. Brancato and James G. Allard, "Effects of Electron Irradiation on the Electrical Properties of Mylar", Power Apparatus and Systems, February 1958, pp. 1539-1545.

27. Source supplied through research sponsored by the U. S. Atomic Energy Commission under contract with the Union Carbide Corporation.

28. R. H. Bube, Photoconductivity of Solids, John Wiley and Sons Inc., New York, New York, 1960.

29. J. Lindmayer, "Current Transients in Insulators", J. Appl. Phys. 36, 1965, p. 196.

REFERENCES (continued)

30. M. Abramovity and I. A. Stegun, eds., Handbook of Mathematical Functions with Formulas, Graphs and Mathematical Tables, NBS Applied Mathematics Series 55, U. S. Government Printing Office, Washington, D. C., 1964.

31. B. P. Burtt, "Absolute Beta Counting," Nucleonics 5, August 1949, p. 28.

32. Melvin Calvin, et al., Isotopic Carbon, New York, John Wiley & Sons, Inc., 1949.

NASA-Langley, 1965